Global Journal of Engineering and Technology Advances
eISSN: 2582-5003
Cross Ref DOI: 10.30574/gjeta
Journal homepage: https://gjeta.com/

(RESEARCH ARTICLE)

Check for updates

Advanced optimization of a two-degree-of-freedom PID controller for air pressure monitoring sensor using a multi-objective genetic algorithm

Adunola Fatai Olatunde [1], Anuoluwapo Emmanuel Dada [1], Joshua Sokowonci Mommoh [2, *], Solomon Obhenbhen Ibharunujele [3], Sani Aminu Shuaibu [4] and Ruby Chinyere Beremeh [1]

[1] *Department of Electrical Electronic Engineering, Nigerian Defence Academy, Kaduna, 800281, Nigeria.*
[2] *Department of Software Engineering, Mudiame University Irrua, 310112 Edo, Nigeria.*
[3] *Department of Electrical &Electronic Engineering, Ambrose Alli University, Ekpoma, Edo, 310101, Nigeria.*
[4] *Department of Electrical Electronic Engineering, Federal Polytechnic Kabo, 704103, Kano, Nigeria.*

Global Journal of Engineering and Technology Advances, 2025, 23(02), 045-076

Publication history: Received on 28 March 2025; revised on 03 May 2025; accepted on 05 May 2025

Article DOI: https://doi.org/10.30574/gjeta.2025.23.2.0081

Abstract

This study investigates the optimization of a 2-Degree-of-Freedom Proportional-Integral-Derivative (2DOF-PID) controller for an air pressure monitoring sensor system using a Multi-Objective Genetic Algorithm (MOGA). The research addresses the common challenge of time delays in real-world control systems, which often stem from sensor latency, actuator dynamics, and signal transmission lags which are factors that compromise system stability and performance. To address this, the system was mathematically modeled using a transfer function to represent the dynamic behavior of the air pressure monitoring sensor, a key component in regulating pneumatic systems. The 2DOF-PID controller was implemented to independently manage reference tracking and disturbance rejection, providing greater control flexibility. The MOGA was employed to fine-tune the controller parameters based on three standard performance indices: Integral of Absolute Error (IAE), Integral of Squared Error (ISE), and Integral of Time-weighted Absolute Error (ITAE). For comparison, other optimization algorithms such as ChASO, GA, MOPSO, and ISCA were also applied. Simulation results demonstrated that the MOGA-optimized controller outperformed all other approaches, achieving superior performance metrics: -82.9% flow disturbance rejection, -76.8% temperature disturbance rejection, 1.24% overshoot, no undershoot, a fast-settling time of 44.25 seconds, and a rise time of 53.2 seconds. These results highlight the MOGA's effectiveness in enhancing the robustness and responsiveness of pneumatic control systems.

Keywords: 2DOF-PID Controller; Multi-Objective Genetic Algorithm (MOGA); Air Pressure Monitoring Sensor; Control System Optimization; Disturbance Rejection Performance

1. Introduction

Pneumatic pressure sensors, commonly known as air pressure sensors, play a vital role in various applications by detecting and measuring pressure variations in pneumatic systems. These sensors are essential for ensuring operational safety, preventing equipment failures, and protecting workers from potential hazards. They are extensively utilized in both mobile and industrial hydraulic applications [1]. Proportional-Integral-Derivative (PID) controllers are widely employed in pneumatic pressure monitoring systems due to their ability to regulate valves, generate analog outputs, and ensure operational safety. By continuously adjusting control outputs based on the process variable (PV) received from the sensor, PID controllers enable automated setpoint tracking, enhancing system stability and performance [2]-[3]. However, real-world control systems often exhibit time delays, which introduce significant challenges in achieving optimal control. These delays can arise from sensor response time, actuator dynamics, or signal propagation, leading to difficulties such as oscillations, stability issues, and reduced control effectiveness. Moreover, poor pressure

* Corresponding author: Joshua Sokowonci Mommoh

management can accelerate equipment deterioration, leading to frequent maintenance requirements and system downtime [4]. This can result in inconsistent actuator behavior, misalignment of mechanical components, and overall degradation of product quality. To mitigate these challenges, there is need for an optimized pressure control strategy that incorporates advanced control algorithms and tuning methodologies, ensuring precise and reliable pressure regulation.

Conventional PID tuning techniques fall into three primary categories: rule-based, model-based, and heuristic/genetic tuning. Rule-based tuning methods, such as Ziegler-Nichols, Cohen-Coon, and Lambda tuning, rely on predefined mathematical relationships to adjust PID parameters [5]-[6]. While these approaches offer simplicity, they often fail to handle large dead times, nonlinear system dynamics, and process variations effectively. Model-based tuning techniques improve upon rule-based methods by incorporating mathematical models of the system for parameter optimization. However, these methods suffer from delayed disturbance rejection, particularly in slow response systems. Heuristic approaches, including genetic algorithms (GAs) and multi-objective optimization methods, have gained traction due to their ability to optimize PID parameters by exploring a broader solution space [7]-[9]. Despite their advantages, conventional single-loop PID controllers may struggle to maintain robust performance in complex systems with varying dynamics and multiple objectives. The Two-Degree-of-Freedom (2DOF) PID controller provides a significant improvement over conventional PID controllers by offering greater flexibility and enhanced control performance. It consists of two distinct control loops: an inner loop that manages rapid system dynamics and an outer loop that focuses on setpoint tracking and slow system dynamics. This dual-loop structure enables independent tuning of fast and slow response components, leading to better disturbance rejection and improved overall stability [10]-[12]. A promising approach to optimizing 2DOF-PID controllers involves the application of multi-objective optimization algorithms such as Multi-Objective Particle Swarm Optimization (MOPSO), Genetic Algorithm (GA), Improved Sine Cosine Algorithm (ISCA), and Chaotic Atom Search Optimization (ChASO). These algorithms use evolutionary computation techniques to determine optimal PID parameter sets while simultaneously considering multiple objectives, including minimizing overshoot, reducing settling time, and enhancing system stability. Each optimization algorithm offers unique advantages in tuning the 2DOF-PID controller. MOPSO enhances traditional PSO by integrating Pareto-based multi-objective strategies to improve solution diversity [13]-[15]. GA employs evolutionary selection mechanisms to generate a broad range of optimal solutions. ISCA refines the standard Sine Cosine Algorithm with adaptive strategies to accelerate convergence and improve optimization accuracy. ChASO strengthens Atom Search Optimization by incorporating chaotic maps, enhancing its exploration and exploitation capabilities for robust and efficient PID tuning [16]-[19]. The optimization process typically involves generating an initial population, evaluating fitness values, selecting high-performing candidates, performing crossover and mutation operations (in the case of GA), and iterating until a convergence criterion is met [20]. This study seeks to compare the performances of MOGA, MOPSO, GA, ISCA, and ChASO in optimizing 2DOF-PID controllers for air pressure monitoring sensors to identify the most effective optimization approach for improving pressure control, mitigating time delays, and enhancing system reliability.

2. Literature Review

This section of the research explores optimization techniques previously employed by scholars for PID controller tuning, focusing on their methodologies and results.

In [21], the application of two degree of freedom (2DOF-PID) controllers in addressing the two-area interconnected power system was explored using PSO algorithm. The researchers formulated a specialized fractional-order control problem tailored specifically for time-delay systems. By evaluating the performance of Fractional-Order PID (FOPID) controllers, they found that the controller could be effectively implemented by approximating the FOPID as a ratio of integer-order polynomials. This approximation transformed the FOPID into a fourth-order discrete transfer function while maintaining an error margin of 10%. While the study highlights the effectiveness of FOPID controllers in handling time-delay systems, it also identifies a limitation in disturbance rejection speed, particularly in slower systems. The performance could be enhanced by employing Genetic Algorithms (GA) and controllers with higher-order derivatives.

The work of [22] explored the use of Integral Model Control (IMC) for tuning PID controllers in systems with time delays. The researchers applied a first-order Pade approximation to derive PID parameters from the IMC approach. They conducted simulations on various transfer function models and nonlinear equations, utilizing a straightforward tuning rule specifically designed for stable and unstable First-Order Plus Time Delay (FOPTD) systems—those with a positive zero and those with a negative zero, respectively. The simulation results provide valuable insights into the effectiveness of this tuning method for PID controllers in time-delay systems with zeros. However, the approach is limited as it only supports PI controller tuning, making it unsuitable for considering parameter derivatives. To achieve improved dynamic performance and greater robustness against variations in process dynamics, including nonlinearities, alternative tuning strategies are necessary.

Research [23] proposed the use of PSO and MOPSO auto tunning a PID controller for robotic manipulator. The study utilized MATLAB simulations to evaluate the dead-time and gain margin of a 2-DOF control system while considering constraints such as maximum position error, maximum joint torque, and oscillation limits. The simulation results indicated a slight decline in robust stability compared to a PI controller without filtering in a time-delay system. This drawback led to a slower disturbance rejection. However, the dynamic performance could be further enhanced by implementing a controller with higher-order derivatives.

[24] Developed 2DOF-PID controller using an improved sine-cosine algorithm for load frequency control of a three-area system with nonlinearity. The research enhanced the controller design process by integrating an uncertainty and disturbance estimator, validating their approach through both simulations and experimental testing. They assessed the effectiveness of their proposed method by comparing it with three established tuning techniques: 2DOF with heuristic tuning, AMIGO, and LQR synthesis methods. In this study, the Improved Sine Cosine Algorithm (ISCA) is introduced as a tuning tool for the load frequency controller in a multi-area system with unequal parameters. Given the slow time response observed, future research could explore incorporating a self-tuning regulator or addressing larger time delays through predictor-feedback delay compensation techniques.

3. Methodology

This section presents the methodology employed for the design, optimization, and evaluation of a 2DOF-PID controller.

3.1. Development of Air pressure monitoring sensor

The design of the air pressure monitoring system was carried out on MATLAB/Simulink environment. To achieve this, two pneumatic Tank 1 and 2 as depicted figure 1 were considered.

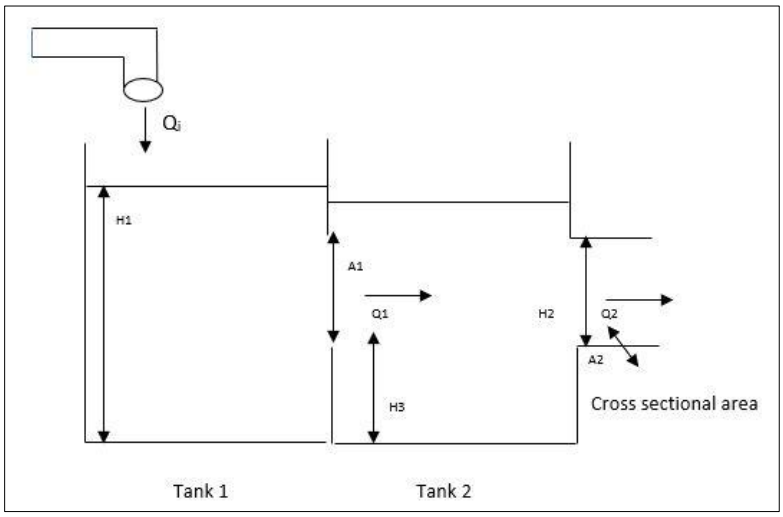

Figure 1 Coupled Pneumatic tank system

By applying Kirchhoff's Voltage Law (KVL) to tank 1 and tank 2, the differential equation presented in equation (1) and (2) were formulated in terms of the pump's input flow rate Q_i and the output flow rate Q_2.

$$Q_i - Q_1 = A\frac{d}{dt}H_1 \quad \ldots\ldots\ldots\ldots \quad (1)$$

$$Q_1 - Q_2 = A\frac{d}{dt}H_2 \quad \ldots\ldots\ldots\ldots \quad (2)$$

Figure 2 illustrates the measured values of the plant at a specific point in time. In this system, Q_i represented the flow rate of the input pump, while Q_1 and Q_2 denoted the output flow rates from Tank 1 (T1) and Tank 2 (T2), respectively. The variables H_1 and H_2 indicated the fluid levels in Tank 1 and Tank 2. K is defined as the proportional gain, and A referred to the cross-sectional area of the tanks. The state-space representation of the coupled tank system, was formulated accordingly. Equations (3) shows the matrix form representation of equation (1) and (2) together.

$$\begin{bmatrix} h_1 \\ h_2 \end{bmatrix} = \begin{bmatrix} \frac{-K_1}{A} & \frac{K_1}{A} \\ \frac{K_1}{A} & \frac{-(K_1+K_2)}{A} \end{bmatrix} \begin{bmatrix} h_1 \\ h_2 \end{bmatrix} + \begin{bmatrix} \frac{1}{A} \\ 0 \end{bmatrix} q_i \qquad \ldots\ldots\ldots\ldots \quad (3)$$

Transfer Function of equation (3) is denoted by equation (4)

$$G(s) = \frac{\frac{1}{K_2}}{\left(\frac{A^2}{K_1K_2}\right)S^2+\left(\frac{A(2(K_1+K_2}{K_1K_2}\right)S+(1)} \ldots\ldots\ldots\ldots \quad (4)$$

The plant measured control parameters at a particular instance of time is depicted by equation (5-7)

$$\text{Actuator} = \frac{0.1}{(3s+1)} \qquad \ldots\ldots\ldots\ldots (5)$$

$$\text{Plant} = \frac{50^{-2s}}{(30s+1)} \qquad \ldots\ldots\ldots\ldots (6)$$

$$G(s) = \frac{5^{-2s}}{90S^2+33S+1} \ldots\ldots\ldots\ldots (7)$$

After multiplying the blocks and PID controller by equation (8), the transfer function of the overall system is presented in equation (9)

$$\frac{C(s)}{R(s)} = \frac{G(s)}{1 + G(s)H(s)} \qquad \ldots\ldots\ldots\ldots (8)$$

$$G_{PID}(s) = \frac{5^{-2s}}{(90)S^2+(33)S+1 + 5^{-2s}} * \left(K_p + \frac{K_I}{S} + \frac{K_{ds}}{\alpha K_{ds}+1}\right) \qquad \ldots\ldots\ldots\ldots (9)$$

Closed Loop Coupled Tank System with unity gain feedback is presented in figure 2. Figure 3 presents the response of an untuned and unoptimized air pressure sensor, along with the corresponding values for each fitness function. It was clearly observed that the ITAE criterion was more effective in minimizing larger errors in the control system compared to the other error metrics.

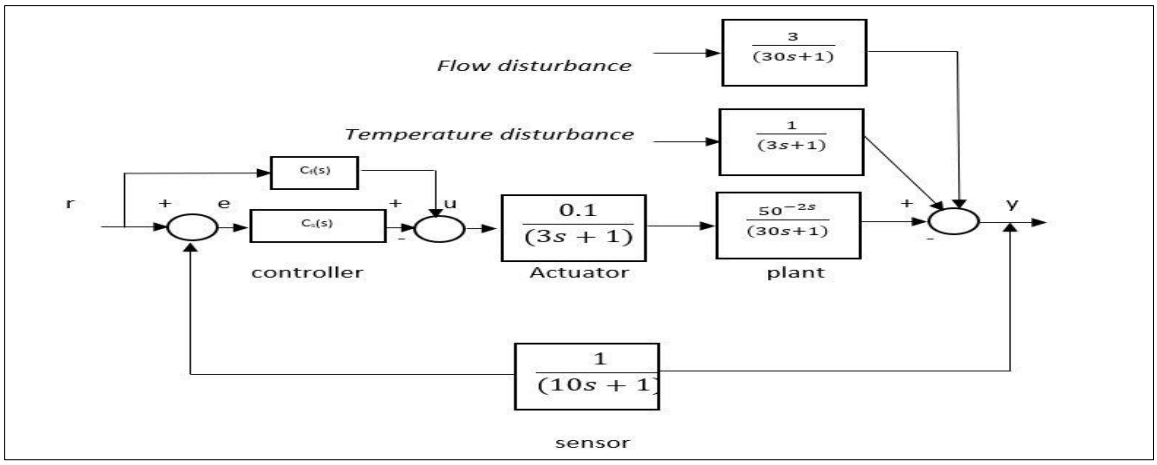

Figure 2 Air pressure with controller and disturbances

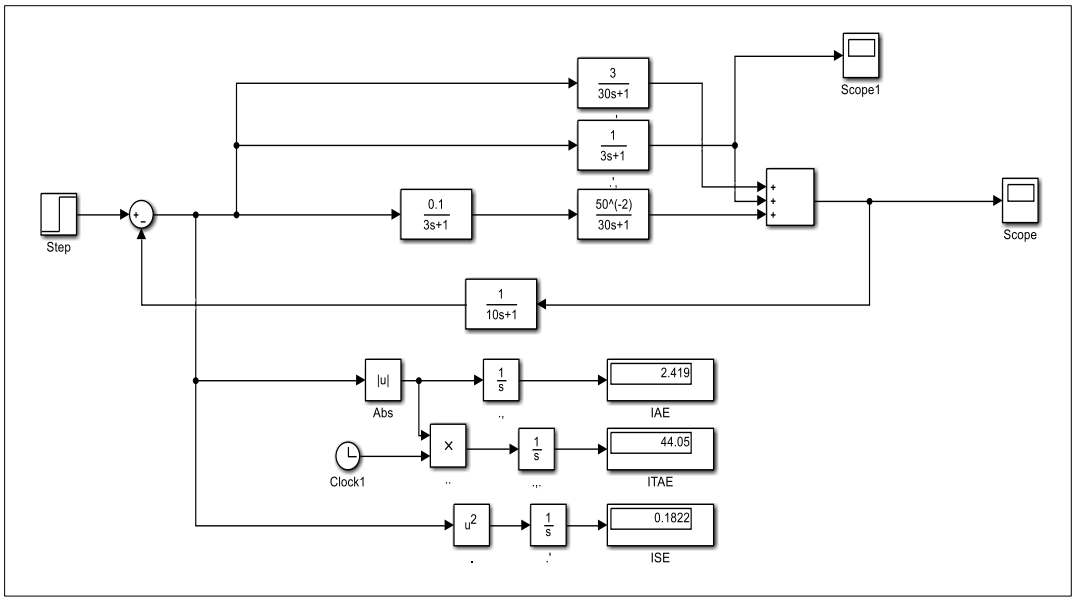

Figure 3 An uncontrolled Simulink block of an air pressure monitoring sensor

3.2. Controller Selection

The 2DOF-PID and 2DOF-PI controllers were considered for this research. The PID controller includes a derivative component, which helps minimize rise time and acts as a damper for the system. However, it can also amplify noise, potentially leading to excessive output from the controller. In contrast, the PI controller is simpler to tune but lacks the derivative component that helps stabilize the plant and reduce the time needed for the controller to minimize error. To assess the performance of both controllers under real-world conditions, they were evaluated in the presence of additional disturbances, such as surface friction. The choice of controller is crucial to meet the pneumatic pressure system's requirements, which involve unpredictable disturbances like surface friction. Both PID and PI controllers, tuned using the MOGA method, were compared in a real-life application to evaluate their suitability for the pressure system. The PID controller was selected as the fixed tuning method for comparison, as it is easier to tune. Initially, the plant was tuned using both PI and PID controllers with MOGA optimization. The step response of the plant, including the controllers, was evaluated, focusing on performance parameters like rise time, overshoot, settling time, and the overall step response graph to detect any fluctuations in the pneumatic readings. Based on experimental data, the 2DOF-PI controller resulted in fluctuating readings, leading to the decision to use the 2DOF-PID controller instead.

3.2.1. Controller Implementation and Configuration

The 2DOF PID Controller block implements a two-degree-of-freedom PID controller (which can be configured as PID, PI, or PD) through the matblab Simulink. It is essentially the same as the Discrete PID Controller (2DOF) block but with the Time Domain parameter set to Continuous-time. The block generates an output signal by calculating the difference between a reference signal and the measured system output. It computes a weighted difference signal for the proportional and derivative actions, based on the specified setpoint weights (b and c). The output of the block is the sum of the proportional, integral, and derivative actions applied to their respective difference signals, each of which is weighted by the corresponding gain parameters P, I, and D, along with a first-order pole. The block supports various controller types and structures. Configurable options available to the user in the block include:

- Controller type (PID, PI, or PD) — Controller parameter.
- Controller form (Parallel or Ideal) — Form parameter.
- Time domain (continuous or discrete) —Time domain parameter.
- Initial conditions and reset trigger —Source and External reset parameters.
- Output saturation limits and built-in anti-windup mechanism —Limit output parameter.
- Signal tracking for bumpless control transfer and multiloop control — Enable tracking mode parameter filters the derivative action.

Figures 4, 5, and 6 illustrate the PID control configuration methods for a closed-loop system used in this research. In this setup, the discrete PID controller measures the error, performs the necessary calculations, and generates the

control input at each sampling interval *T*. The sample time is chosen to be shorter than the system's shortest time constant to ensure accurate control performance.

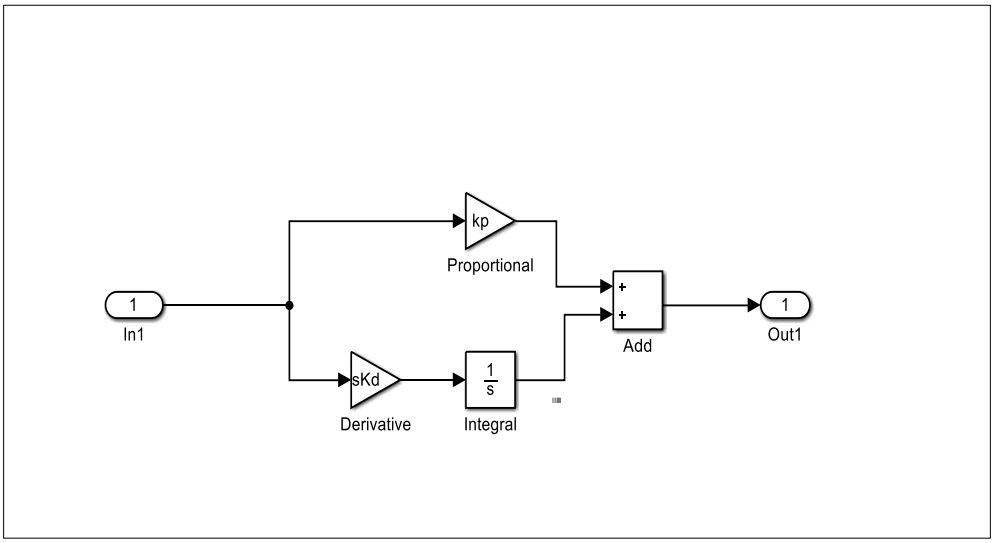

Figure 4 Discrete PID Controller Simulink.

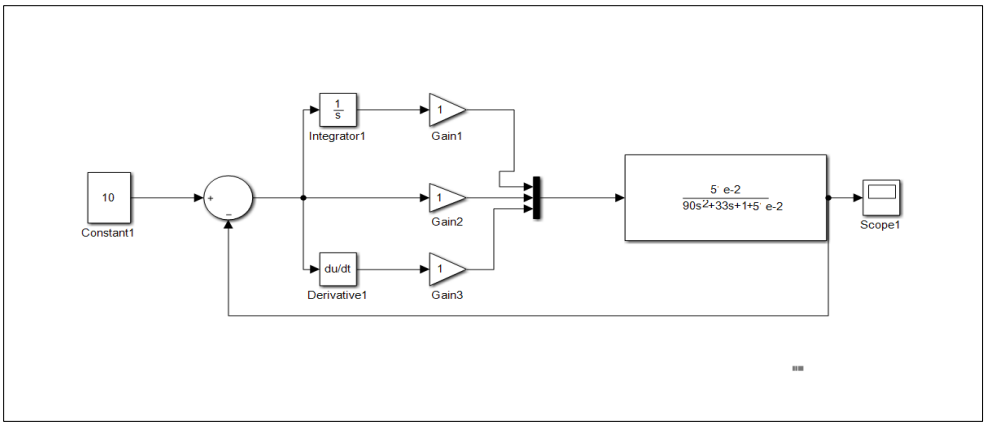

Figure 5 Simulink representation of PID Setpoint Tracking

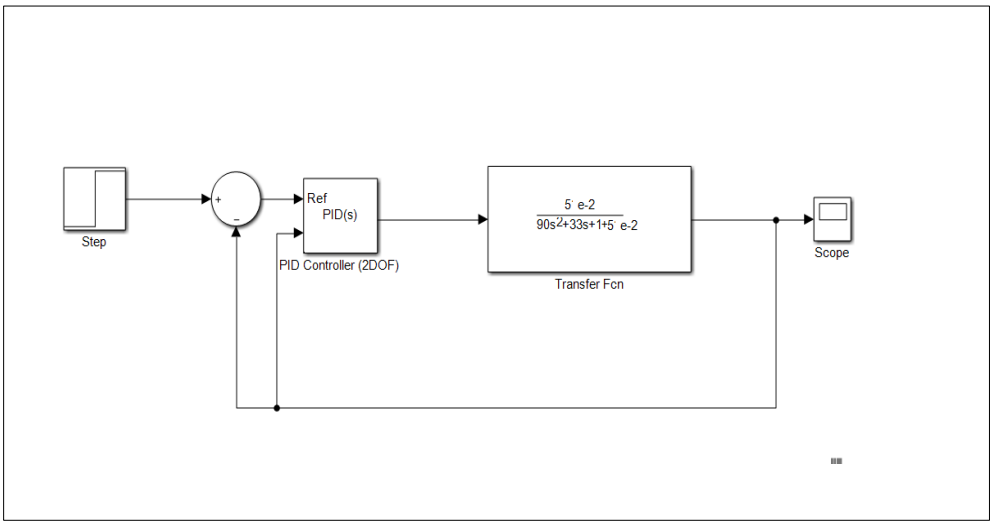

Figure 6 Closed loop system with unity feedback.

3.2.2. DOF-PID Gain Tuning

The PID controller coefficients and setpoint weights can be adjusted either manually or automatically. Automatic tuning necessitates the use of Simulink Control Design software as depicted in figure 7. These PID tuning methods can be applied to control the 2DOF air pressure monitoring system.

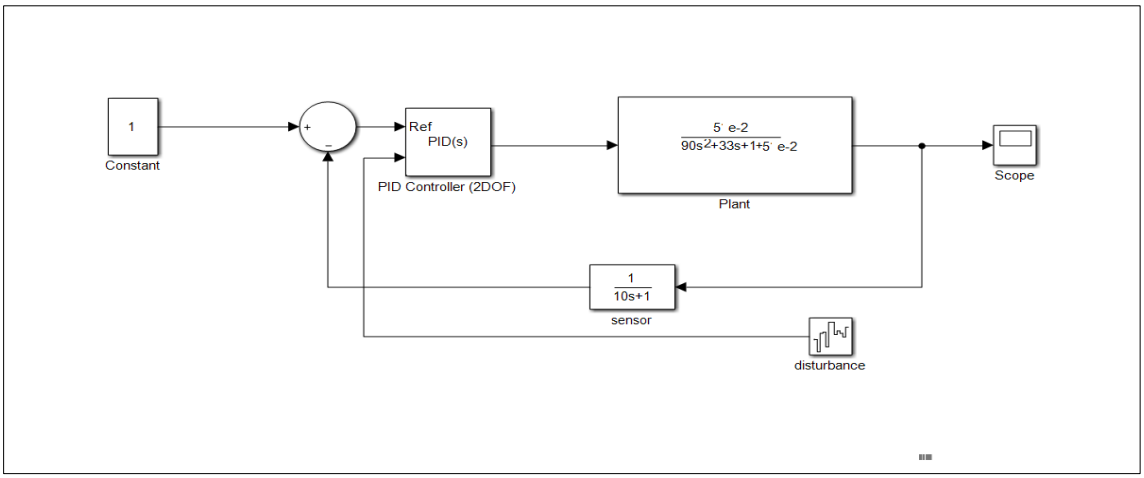

Figure 7 Simulink representation of 2DOF Setpoint Tracking

The 2DOF-PID controller in Simulink can be expressed as mathematically by equation (10).

$$C(s) = P\,(b.r - y) + I\frac{1}{S}(r - y) + D\,\frac{N}{1+N\frac{1}{S}}(c.r - y) \qquad \ldots\ldots\ldots\ldots\ldots \qquad (10)$$

Where, *(N)* denotes Filter coefficient, *(b)* is the first Setpoint weight, and *(c)* is the second setpoint weight.

3.3. Development ISCA -2DOF-PID controller

In this research, the development of the ISCA-2DOF-PID controller was achieved by incorporating the Improved Sine Cosine Algorithm (ISCA). Table 1 following outlines the parameters used in the simulation of the ISCA 2DOF-PID controller for the air pressure sensor.

Table 1 ISCA Parameters

Parameters	**Details**
Population Type	Double Vector
Population Size	500
Low Band	[0]
Upper Band	[500]
Initial Range	[-10 10]
Selection Function	Stochastic uniform
Iteration	500
Crossover Fraction	0.7
Maximum Generation	300

Figure 8 presents a Simulink diagram of the ISCA-2DOF-PID, demonstrating the step-by-step process of how ISCA was implemented in MATLAB. The ISCA was incorporated after simulating the 2DOF-PID controller with the air pressure sensor. The scope shows the step response of the algorithm, while the step info provides performance metrics such as rise time, settling time, overshoot, and undershoot. The fitness functions used for error analysis of the air pressure sensor include IAE, ISE, and ITAE.

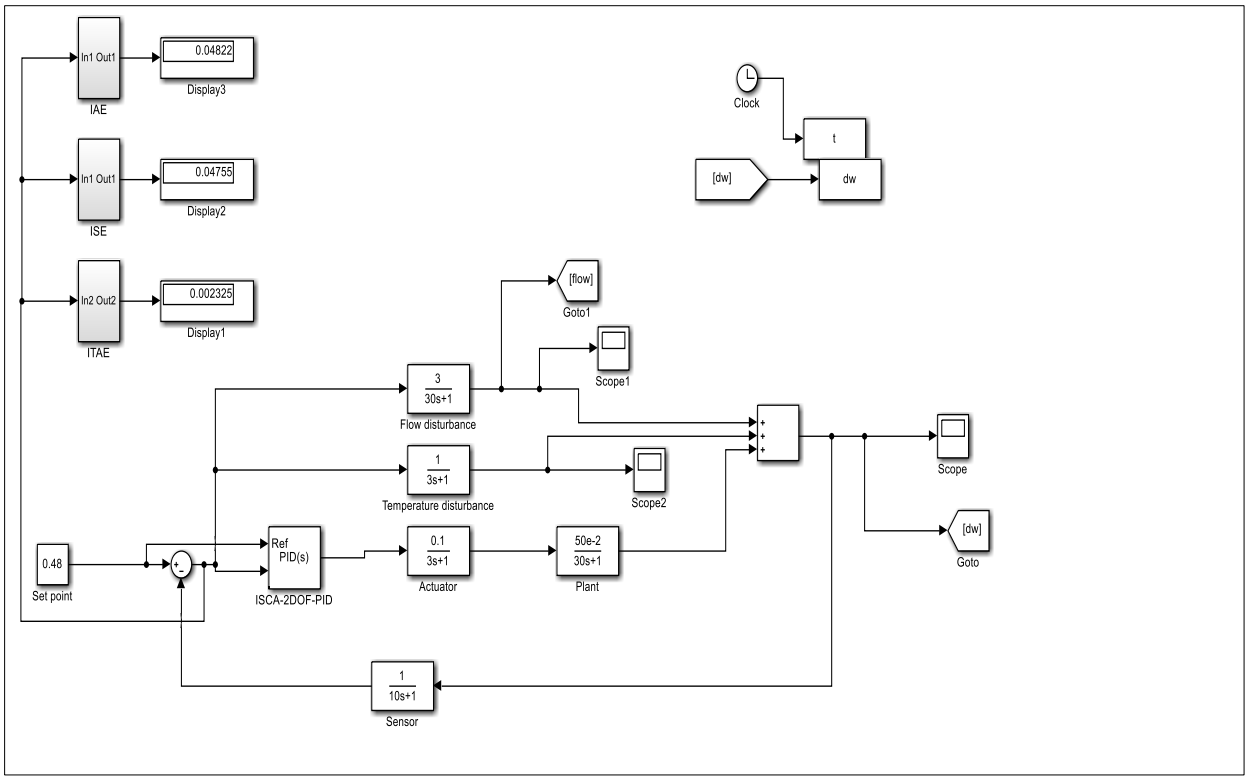

Figure 8 Controlled Simulink model of ISCA-2DOF PID for Air pressure sensor

3.3.1. Implementation of ISCA-2DOF PID optimization process

Algorithm 1: ISCA-2DOF-PID optimization process

Begin ISCA_2DOF_PID_Optimization

Initialize:
Set swarm size, positions [Kp, Ki, Kd], velocities v_i, personal best p_best_i, global best g_best
Set iteration = 0

For iteration = 1 to max_iterations:
Evaluate fitness f(Kp, Ki, Kd) for each particle using 2DOF-PID performance (e.g., IAE, ISE, ITAE)
Update personal best p_best_i if f(Kp, Ki, Kd) < f(p_best_i)

Update particle positions and velocities

Optionally update archive with non-dominated solutions from current swarm
Update global best g_best from archive

If stopping criteria met (e.g., convergence or max_iterations), break

Return best [Kp, Ki, Kd] values as optimized PID parameters

End ISCA_2DOF_PID_Optimization

3.4. Development MOPSO-2DOF PID controller

The design of the MOPSO-2DOF-PID controller was accomplished by integrating Multi-Objective Particle Swarm Optimization (MOPSO) with the two-degree-of-freedom (2DOF) PID controller. Table 2 shows the parameters selected employed in the simulation of the MOPSO-2DOF-PID controller for the air pressure sensor in.

Table 2 MOPSO Parameters

Parameters	Details
Population Type	Double Vector
Population Size	500
Low Band	[0]
Upper Band	[500]
Initial Range	[-10 10]
Selection Function	Stochastic uniform
Iteration	500
Crossover Fraction	0.7
Maximum Generation	300

Figure 9 illustrates the building blocks and performance metrics for the closed-loop control system. Figure 10 presents the Simulink diagram of the MOPSO-2DOF-PID, outlining the step-by-step process of implementing MOPSO in MATLAB. The MOPSO was incorporated after simulating the 2DOF-PID controller with the air pressure sensor. The scope visualizes the step response of the algorithm, while the step info provides performance metrics such as rise time, settling time, overshoot, and undershoot. The fitness functions used for error analysis of the air pressure sensor include IAE, ISE, and ITAE.

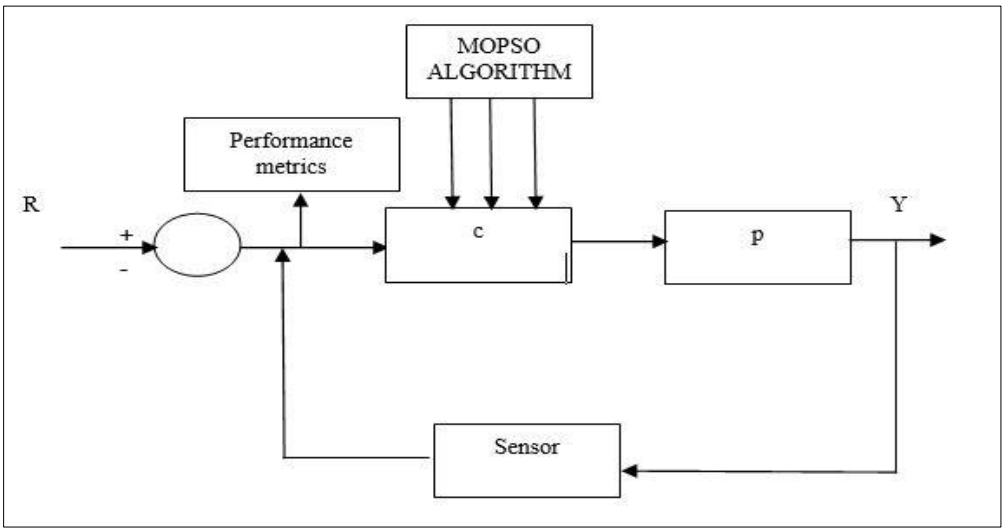

Figure 9 Block diagram of MOPSO process.

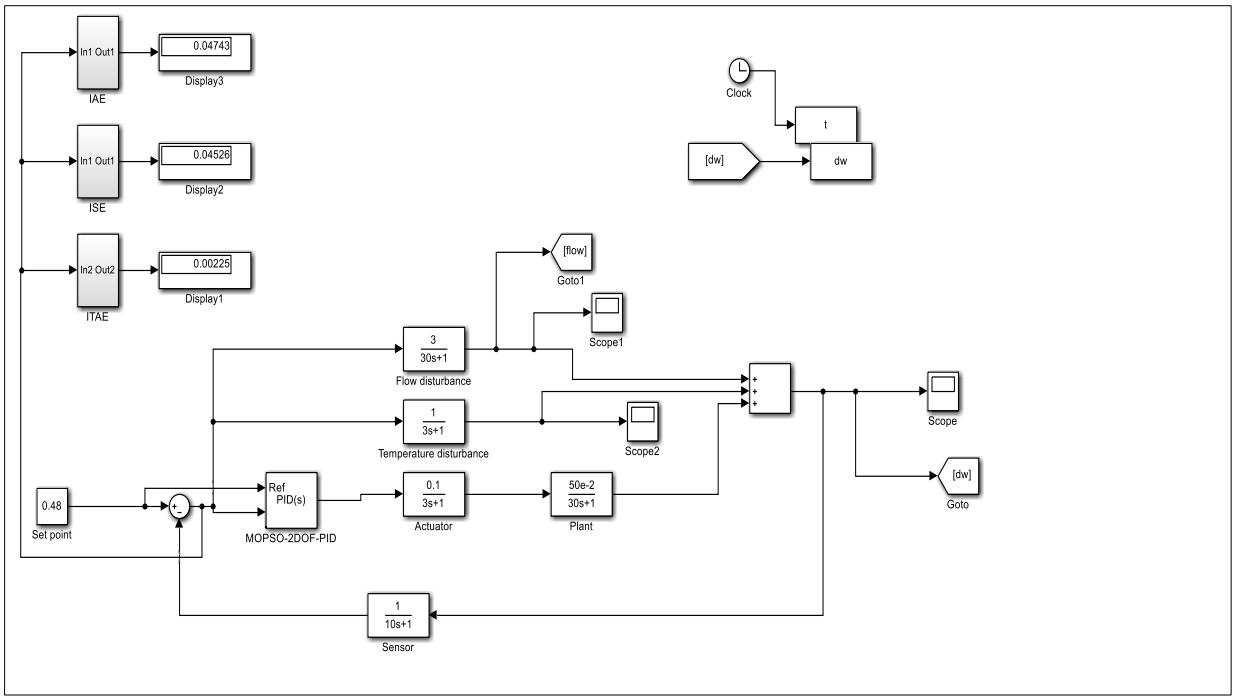

Figure 10 A controlled Simulink model of MOPSO-2DOF PID for Air pressure sensor

3.4.1. Implementation of MOPSO-2DOF PID optimization process

Algorithm 2: MOPSO-2DOF PID optimization process

```
Begin MOPSO_Optimization

 Initialize:
  Set swarm size, positions x_i, velocities v_i, personal best p_best_i, global best g_best
  Set iteration = 0

 For iteration = 1 to max_iterations:
  Evaluate fitness f(x_i) for each particle
  Update personal best p_best_i if f(x_i) < f(p_best_i)

  Update particle positions and velocities

  Optionally update archive with non-dominated solutions, pruning if necessary
  Update global best g_best from archive

  If stopping criteria met, break

 Return final Pareto-optimal solutions

End MOPSO_Optimization
```

3.5. Development of ChASO-2DOF-PID controller

The numerical simulation of the ChASO-2DOF-PID approach involves designing a ChASO-2DOF-PID controller to determine the optimal parameters for the 2DOF-PID controller, which is then compared with other methods. This is achieved by integrating the Chaotic Atom Search Optimization (ChASO) algorithm with the controller in

MATLAB/Simulink. Table 3 outlines the parameters used in simulating the ChASO-2DOF-PID controller for the air pressure sensor.

Table 3 CHASO Parameters

Parameter	Value
Population Size	100
Mutation Fraction	0.1
Inertia weight	0.99
Crossover Fraction	0.8
Lower boundary	0
Upper boundary	100
Iteration	100

Figure 13 presents the Simulink diagram of the ChASO-2DOF-PID, demonstrating the step-by-step process of implementing ChASO in MATLAB. The ChASO algorithm was integrated after simulating the 2DOF-PID controller with the air pressure sensor. The scope visualizes the step response of the algorithm, while the step info provides performance metrics such as rise time, settling time, overshoot, and undershoot. The fitness functions used for error analysis of the air pressure sensor include IAE, ISE, and ITAE.

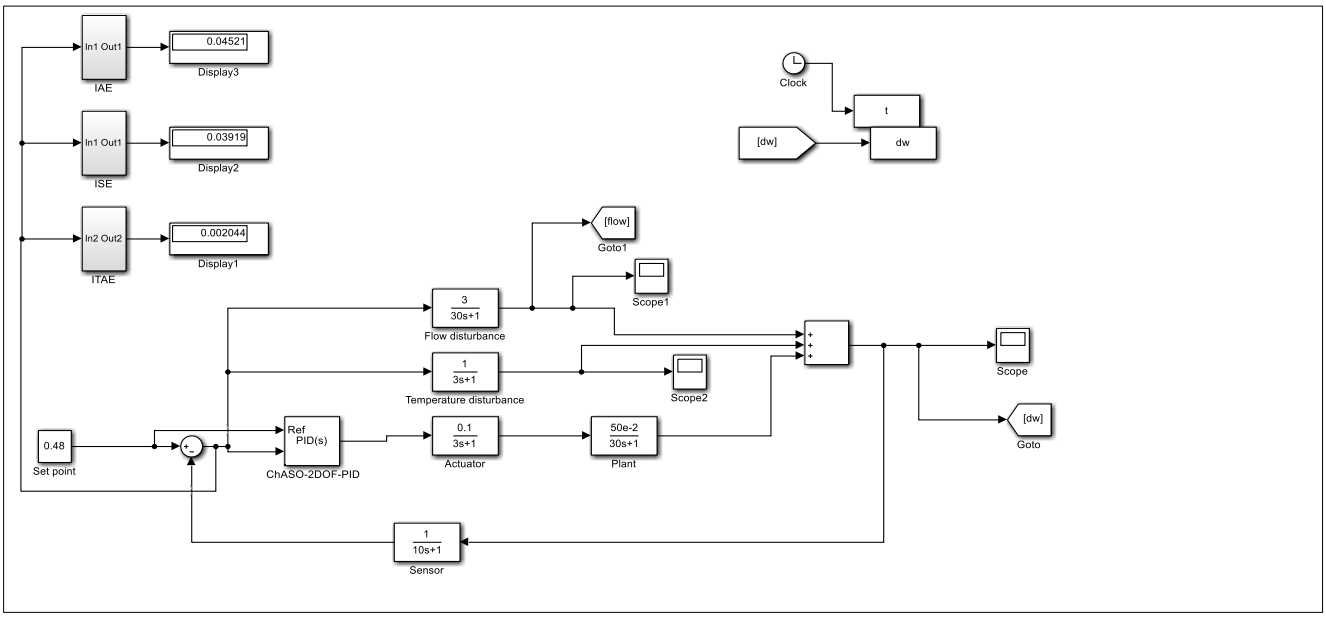

Figure 11 A controlled Simulink model of ChASO-2DOF PID for Air pressure sensor

3.5.1. Implementation of ChASO-2DOF-PID optimization process.

Algorithm 3: ChASO-2DOF-PID optimization process

Begin ChASO_Optimization

Initialize:

Set parameters: num_variables, variable_ranges, population_size, max_iterations, crossover_rate, mutation_rate

Generate initial population randomly within variable_ranges

For iteration = 1 to max_iterations:

```
  Crossover:
    For each parent pair, if r < crossover_rate, perform crossover; else, retain parents

  Mutation:
    For each chromosome, if r < mutation_rate, mutate a random gene

  Chaos:
    For each chromosome, apply logistic map to each gene and update with chaotic value

  Merge & Sort:
    Combine populations, evaluate fitness, sort, and select top `population_size` for next generation

  If stopping criteria met (convergence or max iterations), break

 Return best_solution

End ChASO_Optimization
```

3.6. Development of GA-2DOF-PID controller

The development of the GA-2DOF-PID controller was done by integrating (GA) Genetics algorithm. Table 4 parameters used in the simulation of GA-2DOF-PID controller for an Air pressure sensor.

Table 4 GA Parameters

Parameters	Details
Population Type	Double Vector
Population Size	500
Low Band	[0]
Upper Band	[500]
Initial Range	[-10 10]
Selection Function	Stochastic uniform
Iteration	500
Crossover Fraction	0.7
Maximum Generation	300

Figure 12 presents the Simulink model of the GA-2DOF-PID system, detailing the step-by-step implementation of the Genetic Algorithm (GA) within MATLAB. The GA was incorporated following the simulation of the 2DOF-PID controller with an air pressure sensor. The system's step response is visualized through a scope, while performance metrics such as rise time, settling time, overshoot, and undershoot are displayed using the step info block. For the evaluation of control accuracy, the fitness function was based on error criteria including the Integral of Absolute Error (IAE), Integral of Squared Error (ISE), and Integral of Time-weighted Absolute Error (ITAE).

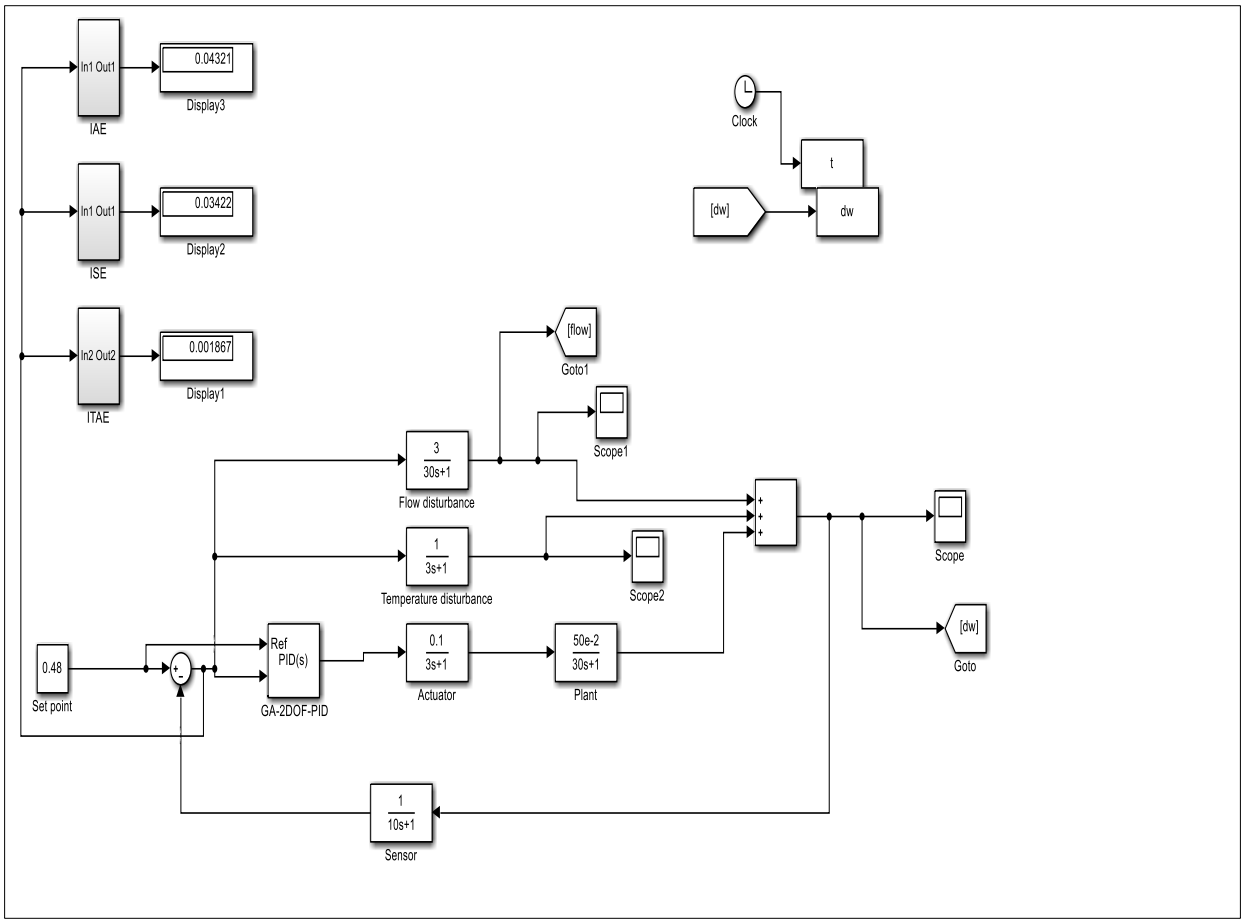

Figure 12 A controlled Simulink model of GA-2DOF PID for Air pressure sensor

3.6.1. Implementation of GA-2DOF-PID optimization process

Algorithm 4: GA-2DOF-PID optimization process

```
Begin GA_2DOF_PID

 Initialize:
   Set population_size, num_generations, crossover_rate, mutation_rate
   Generate initial population with random [Kp, Ki, Kd] within bounds

 For generation = 1 to num_generations:
   Evaluate fitness of each individual (e.g., IAE, ISE, ITAE)
   Select mating pool based on fitness
   Apply crossover to create offspring (with crossover_rate)
   Apply mutation to offspring (with mutation_rate)
   Form new population from offspring
   If convergence or max_generations reached: Break

 Return best [Kp, Ki, Kd]

End GA_2DOF_PID
```

3.7. Development of MOGA-2DOF-PID controller.

The development of the GA-2DOF-PID controller was carried out using a Multi-Objective Genetic Algorithm (MOGA). Table 5 outlines the parameters employed in simulating the MOGA-2DOF-PID controller for the air pressure sensor system.

Table 5 Parameter Setting for MOGA-2DOF-PID

Parameter	Value
Population Size	100
Mutation Fraction	0.1
Inertia weight	0.99
Crossover Fraction	0.8
Lower boundary	0
Upper boundary	100
Iteration	100

The Simulink model of the MOGA-2DOF-PID controller, demonstrating the step-by-step integration of the Multi-Objective Genetic Algorithm (MOGA) in MATLAB is shown in figure 13. The MOGA was incorporated following the simulation of the 2DOF-PID controller with the air pressure sensor. The system's step response is visualized using a scope, while key performance metrics—such as rise time, settling time, overshoot, and undershoot—are displayed via the step info block. For error analysis, the fitness evaluation was based on multiple criteria, including the Integral of Absolute Error (IAE), Integral of Squared Error (ISE), and Integral of Time-weighted Absolute Error (ITAE).

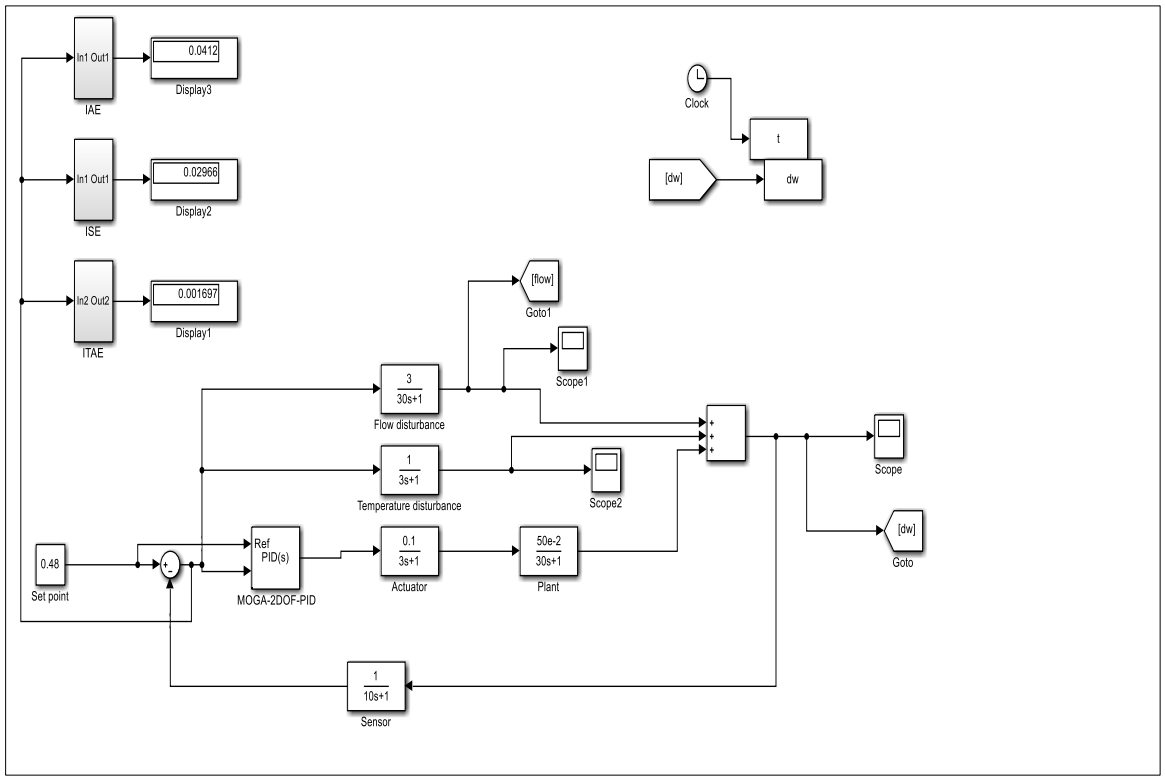

Figure 13 A controlled Simulink model of MOGA-2DOF PID for Air pressure sensor

3.7.1. Implementation of MOGA-2DOF-PID optimization process

Algorithm 5: MOGA-2DOF-PID optimization process
Initialize population with random [Kp, Ki, Kd] Set parameters: population_size, num_generations, crossover_rate, mutation_rate For each generation: Evaluate fitness (e.g., IAE, ITAE) for all chromosomes Select parents based on fitness Apply crossover and mutation to produce offspring Replace old population with offspring If convergence or max generations met: Break Return Pareto-optimal [Kp, Ki, Kd]

In the block diagram shown in Figure 14, the plant error is computed by subtracting the current setpoint from the desired target value. The Multi-Objective Genetic Algorithm (MOGA) is employed to determine the optimal values of the PID controller gains: Kp, Ki, and Kd. The boundary limits for the proportional and integral gains are set as [2, 5] and [0, 1], respectively, while the derivative gain is fixed at zero [0, 0]. Carefully defining these boundaries is crucial for minimizing the optimization time. A large initial population size of 500 is chosen to increase the likelihood of exploring a wide range of output parameters and achieving a more effective solution. Table 6 presents the simulation setup for the MOGA.

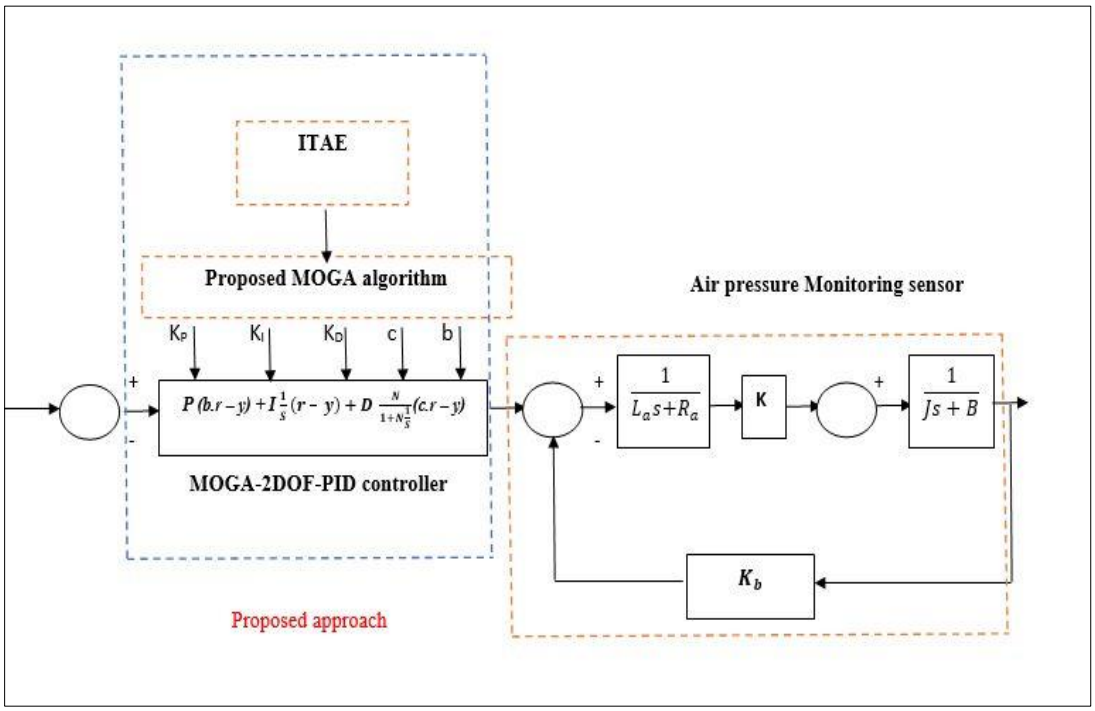

Figure 14 Air pressure monitoring sensor with MOGA-2DOF-PID controller

Table 6 MOGA Simulation Parameters

Parameters	**Details**
Population Type	Double Vector
Population Size	500
Low Band	[0 0]
Upper Band	[2 5]

Initial Range	[-10 10]
Selection Function	Stochastic uniform
Elite Count	2.5
Crossover Fraction	0.7
Maximum Generation	300

4. Result and Discussion

This section discusses the obtained results from the Optimization of a Two-Degree-of-Freedom PID Controller for Air Pressure Monitoring Sensor Using a Multi-Objective Genetic Algorithm. The performance of MOGA, MOPSO, ChASO, GA and ISCA are all compared together for design a 2-DOF PID Controller for Air pressure monitoring sensor in terms of flow and temperature rejection disturbances, rise time, settling time, peak overshoot, undershoot.

4.1. Uncontrolled Selection

Figure 15 illustrates the step response of an air pressure monitoring sensor operating without any controller. As shown, the system fails to reach the desired setpoint, resulting in sluggish dynamics. The step response exhibits a prolonged settling time approximately 320 seconds for flow disturbance rejection and 523 seconds for temperature disturbance rejection. Additionally, the system suffers from significant overshoots, measuring 4.46% for flow and 11.49% for temperature. Even more critically, it experiences substantial undershoots—86.7% in flow and 93% in temperature highlighting poor control characteristics. The performance of the uncontrolled system reflects instability and strong nonlinearity, with a poorly behaved step response. Based on the step response data, the computed fitness function values are also unsatisfactory: IAE of 33.5% (flow) and 28.8% (temperature), ISE of 27.1% (flow) and 11.5% (temperature), and ITAE of 46.2% (flow) and 31.7% (temperature).

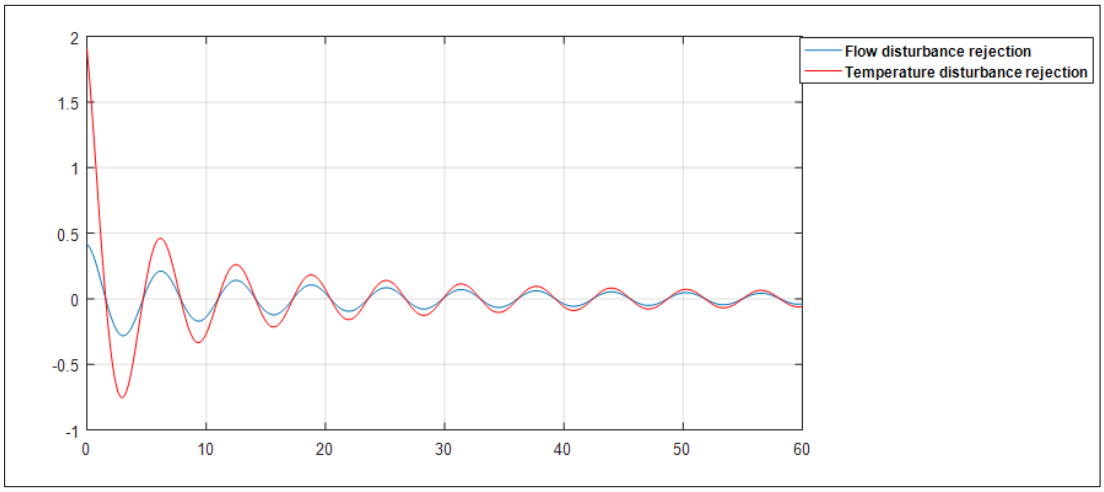

Figure 15 Step response for an uncontrolled system

Based on the results summarized across all tables, the five key parameters of the 2DOF-PID control system K_p ,K_i, K_d, α, β play a crucial role in defining system performance, as explored in the previous section. Among the evaluated fitness criteria, the ITAE (Integral Time-weighted Absolute Error) method proved most effective in minimizing larger errors, demonstrating superior performance in reducing both peak overshoot and disturbances in flow and temperature. Although ITAE takes a longer time to optimize compared to IAE and ISE, its ability to fine-tune parameters for improved transient response makes it a preferred choice. The optimized fitness function values using this algorithm showed significant improvements: IAE at 39.2% (flow) and 30.1% (temperature), ISE at 29.2% (flow) and 14.5% (temperature), and ITAE achieving the best results with 51.1% (flow) and 33.6% (temperature). Mathematically, the Average overshoot, undershoot and percentage reduction are computed using equation (11) – (13)

$$\text{Average overshoots} = \frac{Flow\ overshoot + Temperature\ overshoot}{2} \tag{11}$$

$$\text{Average undershoots} = \frac{Flow\ undershoot + Temperature\ undershoot}{2} \quad (12)$$

$$\%\ \text{Reduction (Temp/Flow)} = \frac{Uncontrolled\ Value - Controlled\ Value}{Uncontrolled\ Value} \times 100 \quad (13)$$

The parameters of controllers C(s) and Cf(s) were simultaneously optimized using the Improved Sine Cosine Algorithm (ISCA) across all three performance criteria. The corresponding fitness function values are illustrated in Figure 8. Among the criteria, ITAE achieved the most significant reduction in flow disturbance. Simulation results, including average overshoot and undershoot, were extracted from the step response analysis. As shown in Table 7, the ITAE value after optimization was notably minimized to 0.002325.

Table 7 Optimized parameters of 2DOF-PID controller simulation using ISCA.

Fitness function criteria for C(S) and C_f(S)	**Value of fitness function**	**Average overshoot For both Flow and Temp.**	**Average undershoots For both Flow and Temp.**	**Reduction Temperature disturbance in (%)**	**Reduction flow disturbance in (%)**
IAE K_p = 0.530 K_i= 0.017 K_d= 3.99 α = 0.011 β = 0.0122	0.04822	0	-0.07	-17.01	-4.5
ISE K_p = 0.830 K_i= 0.047 K_d= 6.79 α = 0.21 β = 0.0462	0.04755	0	-0.06	-7.7	-26.1
ITAE K_p = 0.804 K_i= 0.0454 K_d= 2.76 α = 0.065 β = 0.0112	0.002325	0	-0.04	-10.6	-82.9

The simulated step response data presented in Figures 16 demonstrate highly stable system behavior across all three performance indices. In Figure 16, both IAE and ISE exhibit 0% overshoot and 0% undershoot, while ITAE also shows 0% overshoot with a minimal undershoot of -0.04%. Similarly, in Figure 17, the system maintains 0% overshoot for all criteria, with IAE registering a slight undershoot of -0.07%, ISE at -0.06%, and ITAE once again at -0.04%.

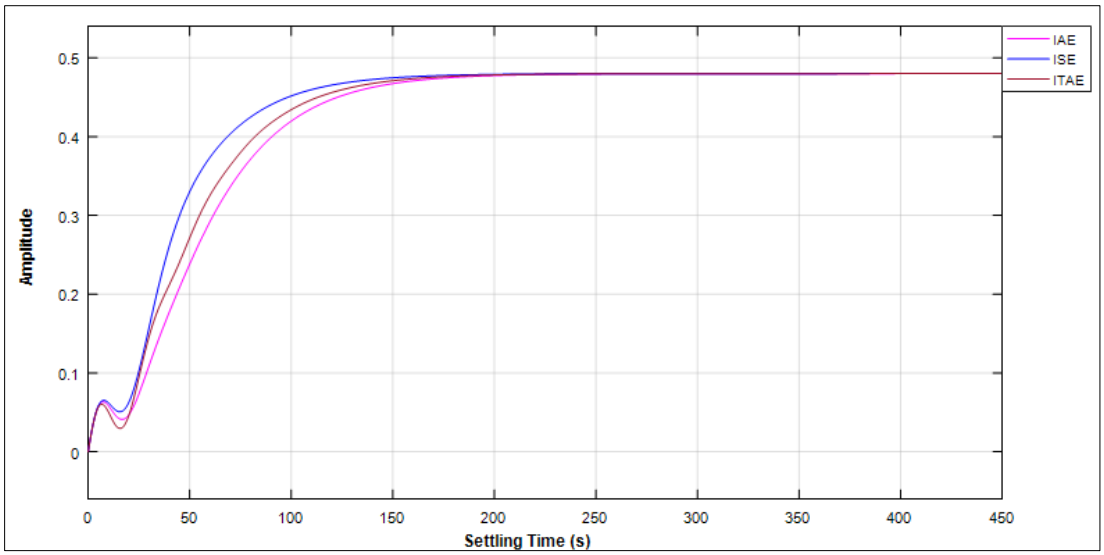

Figure 16 Flow disturbance rejection response with optimization of ISCA-2DOF-PID

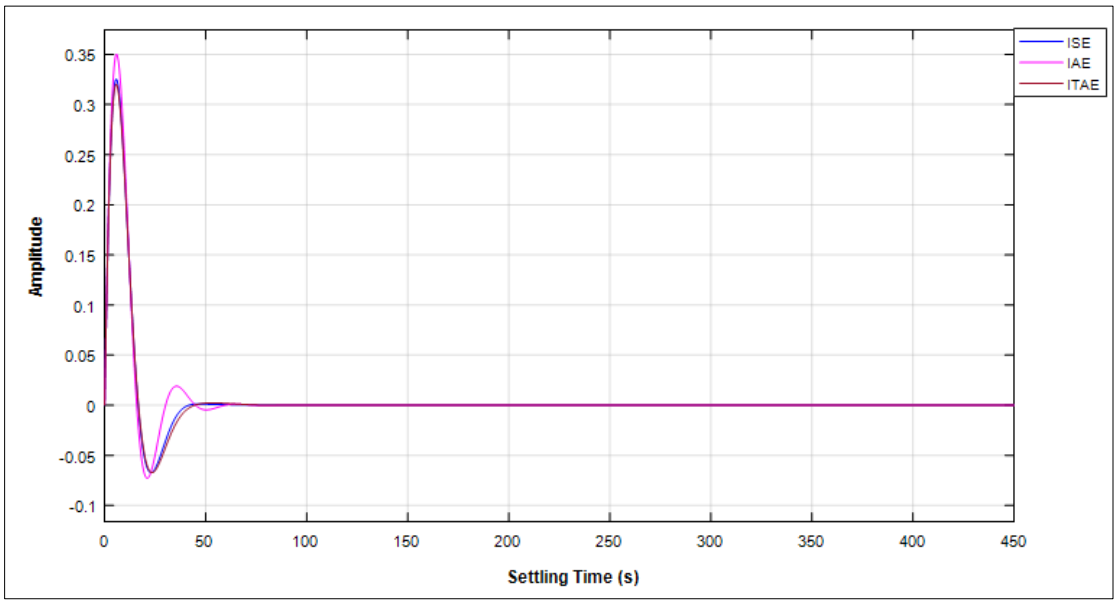

Figure 17 Temperature disturbance rejection response with optimization of ISCA-2DOF-PID

Similarly, all three performance criteria were concurrently optimized for the controller configurations C(S) and Cf (S) using the ISCA algorithm. Among them, the ITAE criterion delivered the most significant reduction in temperature disturbance. It is important to note that the anticipated flow disturbance output from the plant is approximately 0.48, as illustrated in Figure 18.

Based on the results presented in Figures 16 and 17, along with the parameters listed in Table 7, it can be concluded that the ITAE criterion, when applied to optimize all five parameters of the 2DOF-PID controller simultaneously using the ISCA method, achieves the lowest peak overshoot in the step response. However, it requires more time to stabilize the response and optimize the parameters compared to the ISE and IAE criteria. The ITAE criterion also leads to the highest reduction in disturbances, with flow disturbance reduced by 82.9% and temperature disturbance reduced by 10.6%.

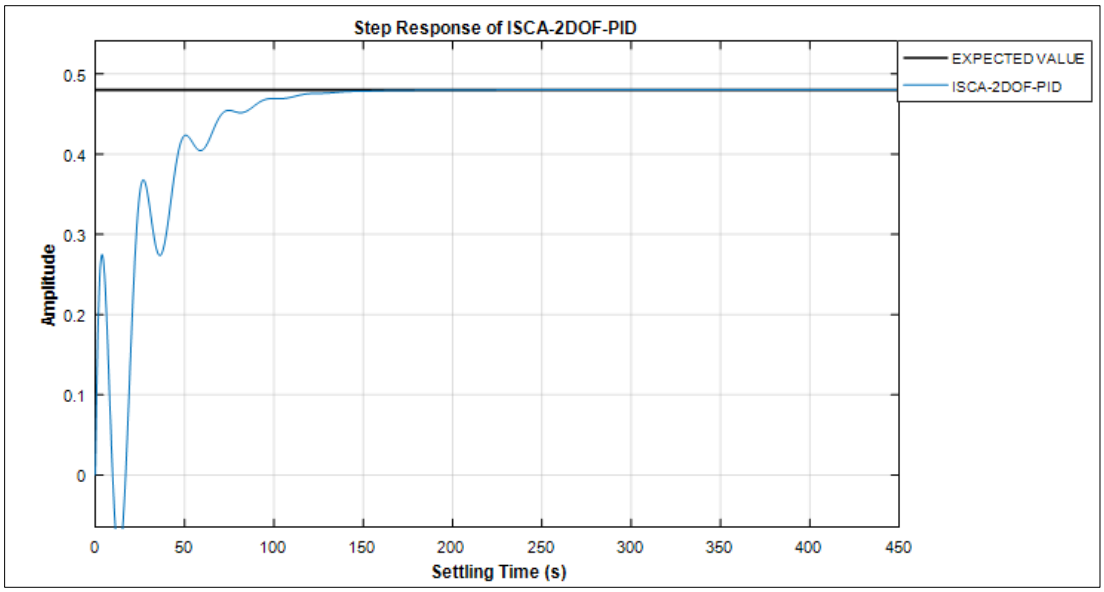

Figure 18 Step Response of ISCA-2DOF-PID

Figure 18 illustrates the behavior of the plant, with the Step info providing the step-response characteristics for the modeled algorithm, as depicted in Figure 8. The ISCA-2DOF-PID controller exhibits a peak value of 0.464, with no overshoot but a significant undershoot of 64.5%. The system achieves a settling time of 143.84 seconds and a rise time of 184.5 seconds.

4.2. Optimized Parameters of MOPSO-2D0F-PID controller

As shown in Table 8 and derived from the data in Figure 10, it is evident that the ITAE criterion performs best for optimizing parameters under various fitness functions, achieving the lowest peak overshoot in the step response and the greatest reduction in both flow and temperature disturbances. While it requires more time to optimize the error parameters compared to IAE and ISE, ITAE proves to be the most effective. The controlled fitness function values for this algorithm, based on step info, are as follows: IAE (26.6% for flow, 39.2% for temperature), ISE (29.4% for flow, 25.3% for temperature), and ITAE (39.6% for flow, 47.4% for temperature).

Table 8 Optimized parameters of 2DOF-PID controller simulation using MOPSO

Fitness function criteria for C(S) and C_f(S)	**Value of fitness function**	**Average overshoot For both Flow and Temp.**	**Average undershoots For both Flow and Temp.**	**Reduction Temperature disturbance in (%)**	**Reduction flow disturbance in (%)**
IAE K_p = 0.5647 K_i= 0.0354 K_d= 1.566 α = 0.0354 β = 0.01568	0.04743	0	-0.049	-17.01	7.6
ISE K_p = 0.830 K_i= 0.047 K_d= 6.79 α = 0.21 β = 0.0462	0.03422	0	-0.055	6.6	-155

ITAE K_p = 0.804 K_i= 0.0454 K_d= 2.76 α = 0.065 β = 0.0112	0.00225	0	-0.032	-2.6	24.9

Using MOPSO, the controller parameters for both C(S) and Cf(S) were simultaneously optimized based on all three performance criteria. The corresponding fitness function values are illustrated in Figure 10. Among the criteria, ITAE yielded the most significant reduction in flow disturbance. The step response data was analyzed to assess the average overshoot and undershoot across the three approaches. According to the step info in Figure 19, both IAE and ISE exhibited 0% overshoot and 0% undershoot, while ITAE also showed no overshoot with a slight undershoot of -0.04%. Similarly, in Figure 20, IAE recorded 0% overshoot with -0.049% undershoot, ISE had 0% overshoot and -0.055% undershoot, and ITAE maintained 0% overshoot with a minimal undershoot of -0.032%.

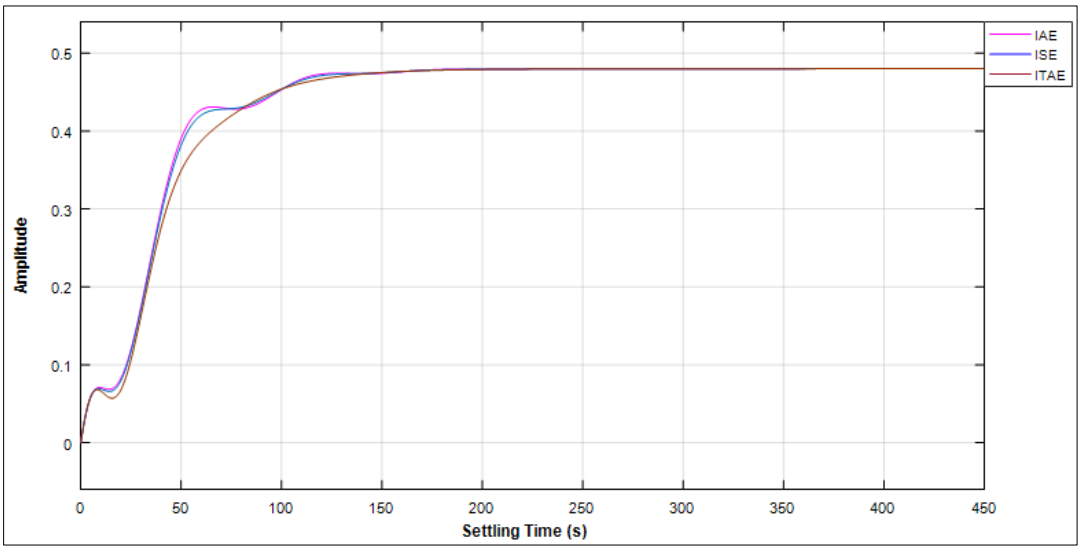

Figure 19 Flow disturbance rejection response optimization of MOPSO-2DOF-PID

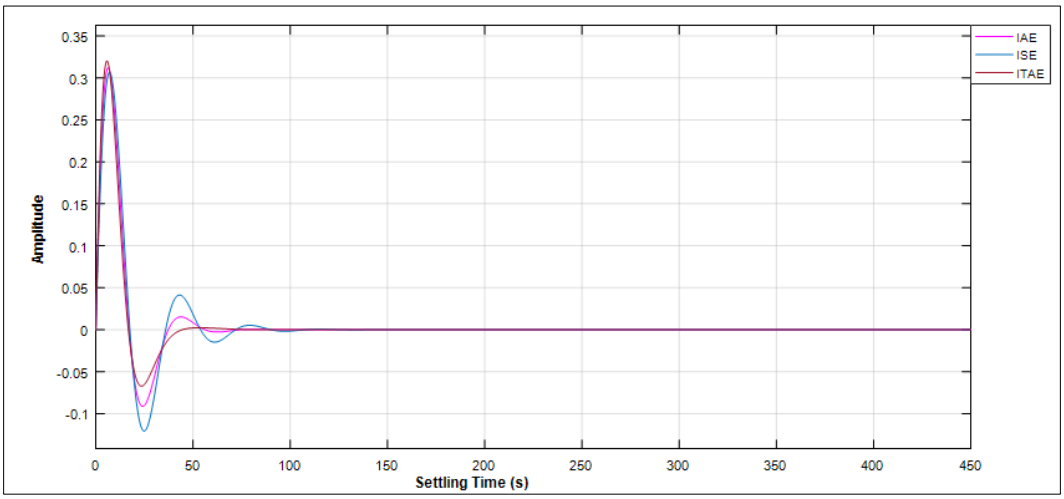

Figure 20 Temperature disturbance rejection response optimization of MOPSO-2DOF-PID

Figure 21 illustrates how the step response characteristics of the modeled system can be analyzed using Step Info to better understand the plant's behavior. The MOPSO-2DOF-PID controller demonstrates a peak response of 0.526, with an overshoot of 8.33% and an undershoot of 11.45%. The system achieves a settling time of 98.34 seconds and a rise time of 88.5 seconds.

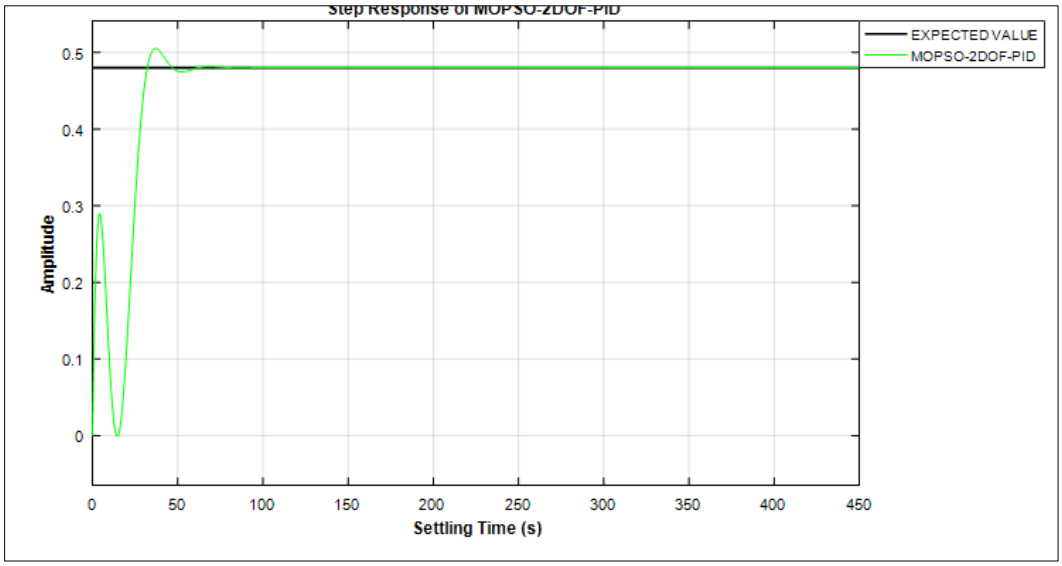

Figure 21 Step Response of MOPSO-2DOF-PID

4.3. Optimized Parameters of GA-2D0F-PID controller

Based on the data summarized in Table 9, the ITAE criterion demonstrates the most effective performance in parameter optimization across multiple fitness functions. It yields the lowest peak overshoot in the step response, along with the highest reduction in flow and temperature disturbances. However, this method also requires more time to fine-tune error parameters compared to the IAE and ISE criteria. According to the step response analysis, the optimized fitness function values using this approach are: IAE (48.7% for flow, 40.3% for temperature), ISE (19.3% for flow, 22.9% for temperature), and ITAE (55.1% for flow, 79.3% for temperature).

Table 9 Optimized parameters of 2DOF-PID controller simulation using GA

Fitness function criteria for C(S) and C_f(S)	**Value of fitness function**	**Average overshoot For both Flow and Temp.**	**Average undershoots For both Flow and Temp.**	**Reduction Temperature disturbance in (%)**	**Reduction flow disturbance in (%)**
IAE K_p = 0.234 K_i= 0.0876 K_d= 1.554 α = 0.062 β = 0.01578	0.04321	0	-0.125	-20.2	-69.1
ISE K_p = 0.0986 K_i= 0.085 K_d= 8.74 α = 0.44 β = 0.654	0.03422	0	-0.179	15.4	-67.8

ITAE K_p = 0.780 K_i= 0.067 K_d= 2.01 α = 0.0677 β = 0.0987	0.001867	0	-0.1	-71.6	-73.8

Likewise, the Genetic Algorithm (GA) is employed to concurrently optimize the parameters of controllers C(S) and Cf(S) based on all three performance criteria. The corresponding fitness function values are illustrated in Figure 12. Among the criteria, ITAE achieves the most significant reduction in flow disturbance. Step response simulation data was used to calculate the average overshoot and undershoot. According to the results in Figure 22, explain the flow disturbance rejection in the control system, ITAE shows the best error rejection -73.8 % in terms of flow. both IAE and ISE exhibit 0% overshoot and 0% undershoot, while ITAE shows 0% overshoot and a slight undershoot of -0.04%. Similarly, Figure 23 reveals that IAE registers 0% overshoot with -0.125% undershoot, ISE shows 0% overshoot with -0.179% undershoot, and ITAE maintains 0% overshoot with a -0.1% undershoot.

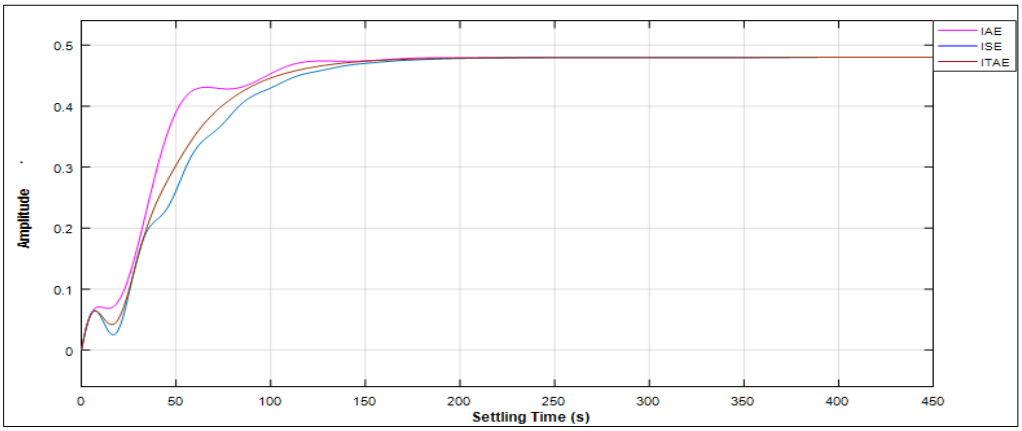

Figure 22 Flow disturbance rejection response optimization of GA-2DOF-PID

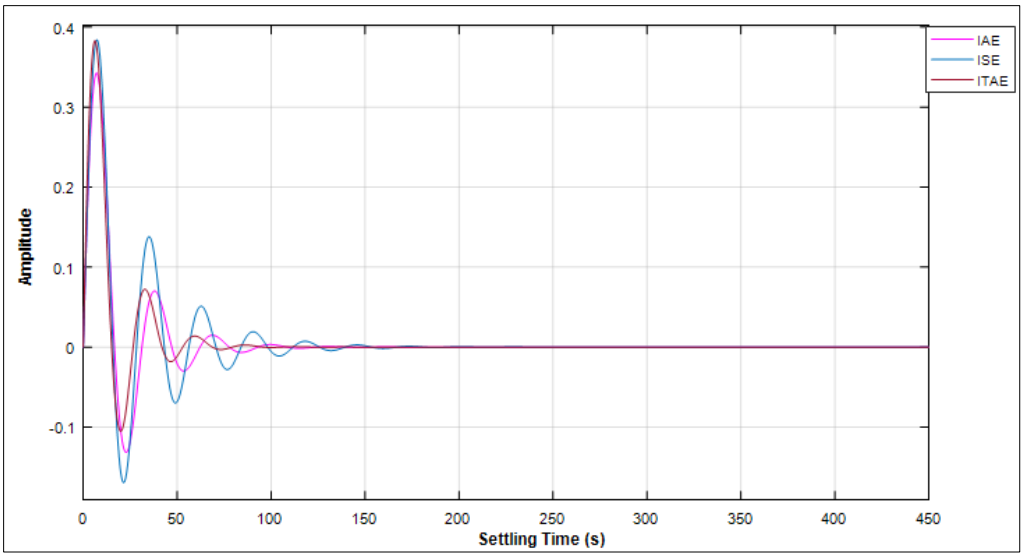

Figure 23 Temperature disturbance rejection response optimization of GA-2DOF-PID

Additionally, ITAE demonstrates the most effective temperature disturbance rejection at -71%. When all five parameters of the 2DOF-PID controller are simultaneously optimized using the MOPSO technique, the ITAE criterion delivers the highest reduction in both flow and temperature disturbances, while maintaining a minimal peak overshoot in the step response.

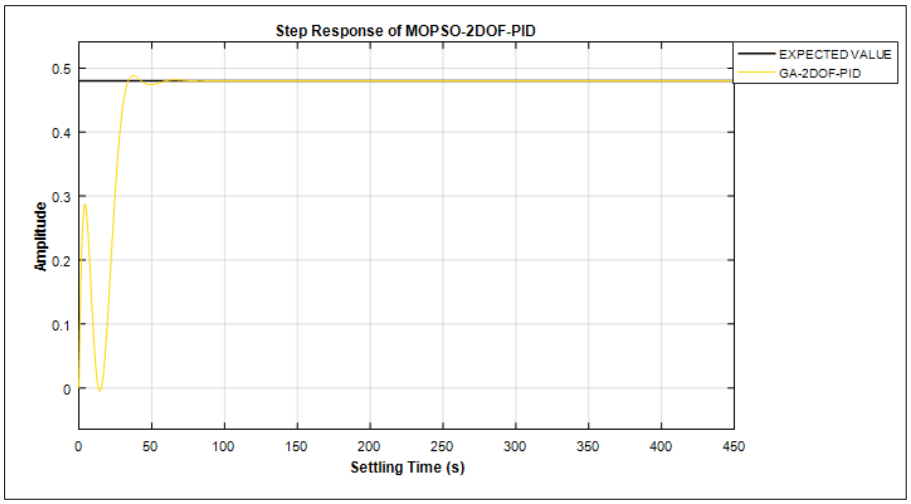

Figure 24 Step Response of GA-2DOF-PID

Figure 24 demonstrates how Step response can be employed to analyze the step-response characteristics of the modeled algorithm, providing insights into the plant's behavior. The GA-2DOF-PID controller exhibits a peak response of 0.491, with an overshoot of 2.46%, no undershoot, a rise time of 79.3 seconds, and a settling time of 66.78 seconds.

4.4. Optimized Parameters of ChASO-2D0F-PID controller

The results presented in Table 10 highlight that the ITAE criterion delivers the most effective parameter optimization across different fitness functions, characterized by the lowest temperature disturbance, the highest reduction in flow deviation, and the smallest peak overshoot in the step response. Compared to ITAE, the IAE and ISE criteria offer faster convergence but less comprehensive error minimization. The five parameters—K_p ,K_i, K_d, α, β —represent key components of the 2DOF-PID control system, as illustrated in the simulation shown in Figure 11. According to the step response data, the controlled fitness function values for this algorithm are: IAE (46.1% flow, 19.2% temperature), ISE (14.9% flow, 28.1% temperature), and ITAE (48.3% flow, 51.6% temperature).

Table 10 Optimized parameters of 2-DOF-PID controller simulation using CHASO

Fitness function criteria for C(S) and C_f(S)	**Value of fitness function**	**Average overshoot For both Flow and Temp.**	**Average undershoots For both Flow and Temp.**	**Reduction Temperature disturbance in (%)**	**Reduction flow disturbance in (%)**
IAE K_p = 0.4544 K_i= 0.0854 K_d= 3.345 α = 0.056 β = 0.0144	0.04521	0	-0.45	73.8	-60
ISE K_p = 0.0345 K_i= 0.0334 K_d= 8.72 α = 0.12 β = 0.344	0.03919	-0.125	-0.1	-3.7	-29.6
ITAE					

K_p = 0.222 K_i= 0.0233 K_d= 6.23 α = 0.044 β = 0.0987	0.002044	0	-0.03	-11.6	-52.3

For all three performance criteria, the ChASO algorithm is applied to simultaneously optimize the parameters of controllers C(S) and Cf (S). The corresponding fitness function values are illustrated in Figure 11, with ITAE achieving the most substantial reduction in flow disturbance. The step response simulation data was used to evaluate the average overshoot and undershoot for each criterion. As shown in Figure 25, IAE records 0% overshoot with a minor undershoot of -0.23%, ISE shows 0% overshoot and -0.05% undershoot, while ITAE also maintains 0% overshoot with a slight undershoot of -0.04%. Similarly, in Figure 26, IAE displays 0% overshoot and -0.67% undershoot, ISE maintains 0% overshoot with -0.1% undershoot, and ITAE continues to show 0% overshoot with only -0.03% undershoot.

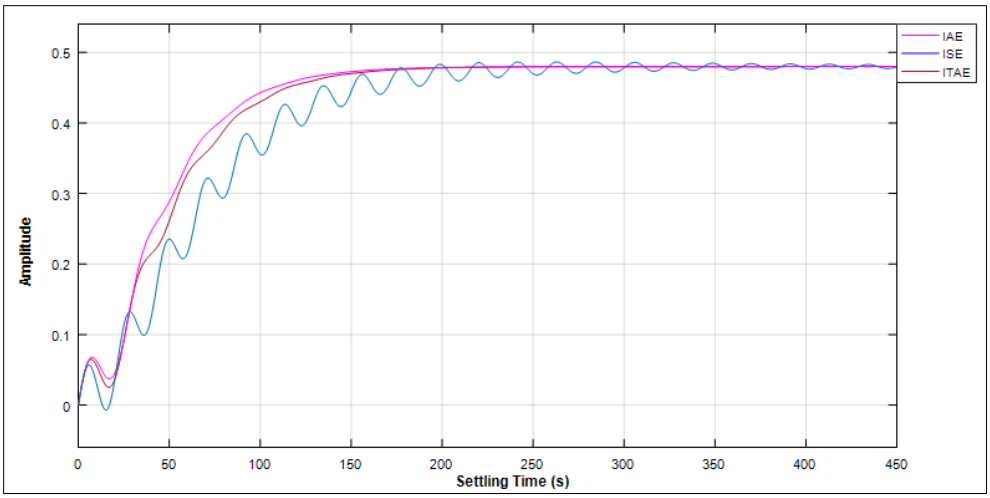

Figure 25 Flow disturbance rejection response optimization of ChASO-2DOF-PID

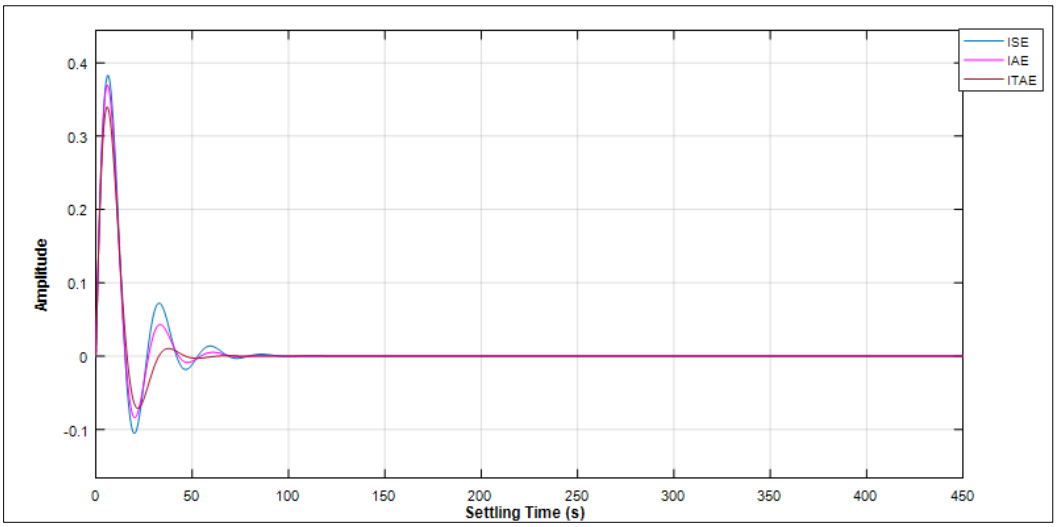

Figure 26 Temperature disturbance rejection response optimization of ChASO-2DOF-PID

As illustrated in Figure 27, the step-response characteristics derived from the step information provide valuable insights into the plant's behavior. The ChASO-2DOF-PID controller demonstrates a well-regulated response, exhibiting

no overshoot and an undershoot of 45.5%. The system reaches a peak value of 0.476, with a rise time of 147.2 seconds and a settling time of 84.33 seconds, reflecting a stable and controlled performance.

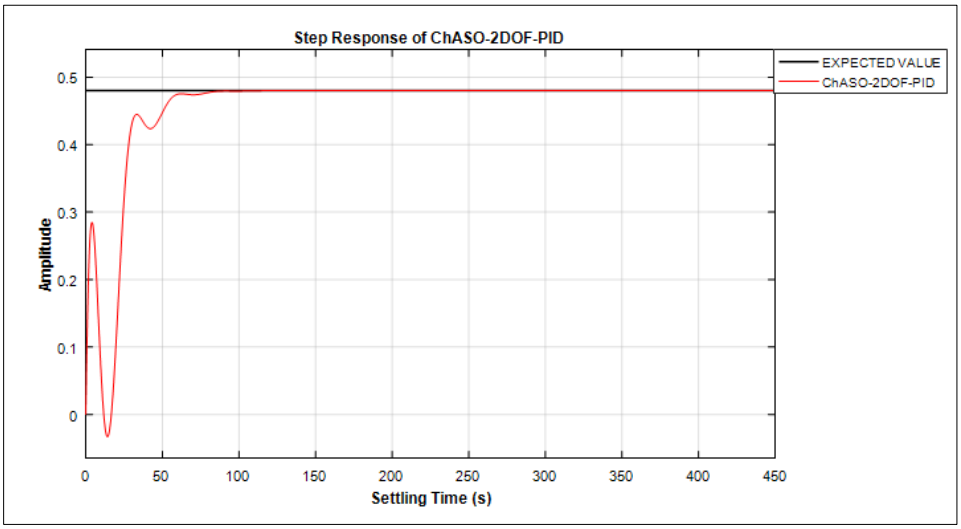

Figure 27 Step Response of ChASO-2DOF-PID

4.5. Optimized Parameters of MOGA-2D0F-PID controller

Figure 30 and Table 11 present the step response analysis of the algorithms implemented in this study, specifically utilizing the MOGA-2DOF-PID controller in conjunction with an air pressure monitoring sensor under varying conditions. The step response was evaluated using different optimization algorithms to assess key performance metrics such as rise time, settling time, overshoot, undershoot, peak value, and peak time. For this research, ITAE, IAE, and ISE were employed as fitness functions. Based on the tabulated results, it is clear that the ITAE criterion consistently delivers superior performance by effectively minimizing larger errors in multi-objective optimization scenarios. Moreover, ITAE demonstrates a greater capacity for reducing both flow and temperature disturbances across the tested conditions. The five key controller parameters—K_p ,K_i, K_d, α, β were simultaneously tuned within the 2DOF-PID framework as shown in Figure 13. According to the step response data, the fitness function outcomes for this algorithm are: IAE (50.7% reduction in flow, 43.4% in temperature), ISE (19.4% in flow, 42.1% in temperature), and ITAE (58% in flow, 81.7% in temperature), further reinforcing ITAE's effectiveness in handling dynamic disturbances.

Table 11 Optimized parameters of 2-DOF-PID controller simulation using MOGA

Fitness function criteria for C(S) and C_f(S)	**Value of fitness function**	**Average overshoot For both Flow and Temp.**	**Average undershoots For both Flow and Temp.**	**Reduction Temperature disturbance in (%)**	**Reduction flow disturbance in (%)**
IAE K_p = 0.354 K_i= 0.0112 K_d= 3.789 α = 0.1432 β = 0.0098	0.0412	0.523	0	-29.5	-76.04
ISE K_p = 0.01312 K_i= 0.0090 K_d= 8.899 α = 0.1098	0.02966	0.02	0	-55.3	-68.6

β = 0.6778					
ITAE K_p = 0.222 K_i= 0.0233 K_d= 6.23 α = 0.044 β = 0.0987	0.001697	0.481	0	-76.8	-82.9

The simulated step response data in Figure 28 shows that for IAE, the overshoot is 0.523% with no undershoot, for ISE the overshoot is 0.493% with no undershoot, and for ITAE the overshoot is 0.481% with no undershoot. Similarly, in Figure 29, IAE exhibits 0% overshoot and no undershoot, ISE shows 0% overshoot and a negligible undershoot of -0%, while ITAE demonstrates 0% overshoot and no undershoot.

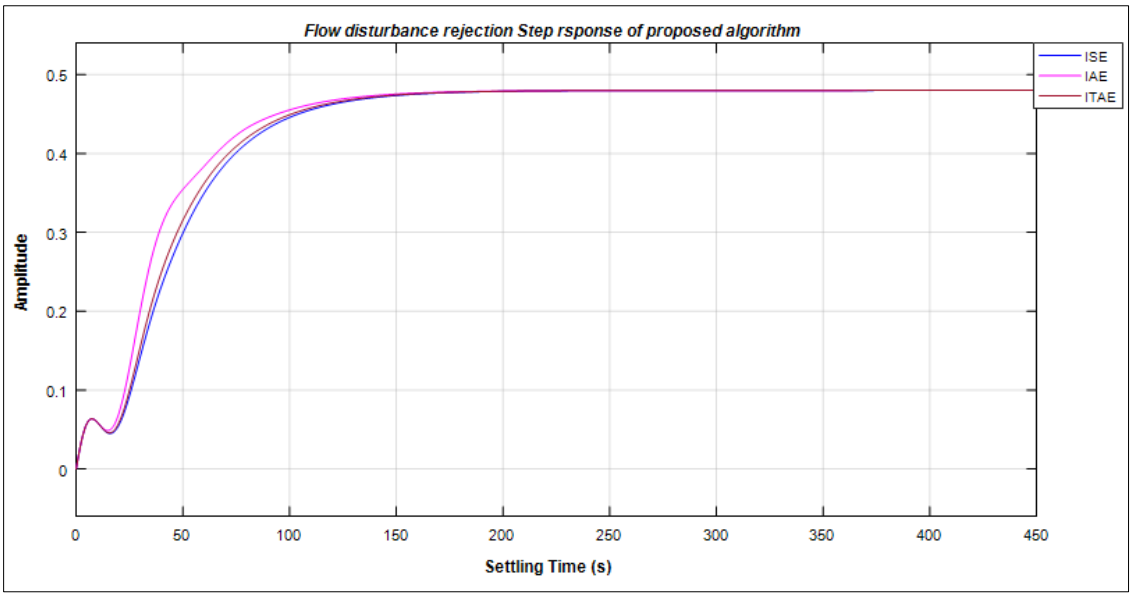

Figure 28 Flow disturbance rejection response optimization of MOGA-2DOF-PID

From Figure 29, ITAE gives the best flow disturbance rejection of -82.9%, likewise in Figure 30, ITAE algo gives the best temperature rejection disturbance of -76.8%.

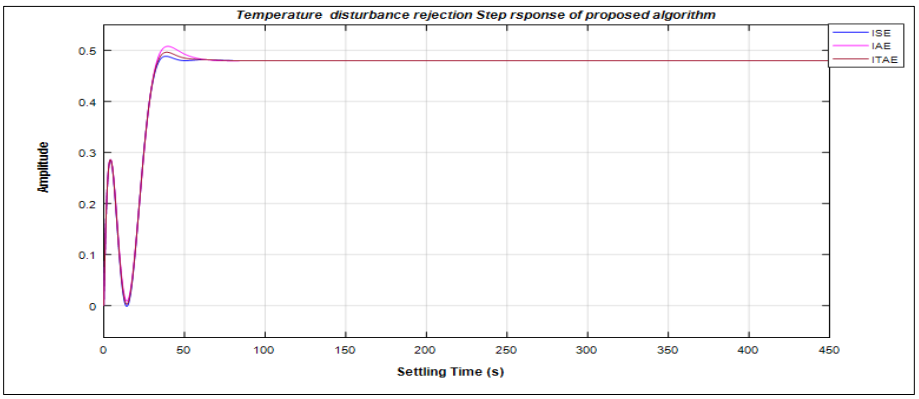

Figure 29 Flow disturbance rejection response optimization of MOGA-2DOF-PID

Additionally, as a key aspect of the objective function, the goal is to achieve the maximum reduction in both flow and temperature across various error criteria. The plant's responses are depicted in Figure 30. Figure 30 illustrates the step-response characteristics of the modeled algorithm, helping to understand the plant's behavior. The MOGA-2DOF-PID (proposed) shows a peak value of 0.485, with a 1.24% overshoot, no undershoot, a settling time of 44.25 seconds, and a rise time of 53.2 seconds.

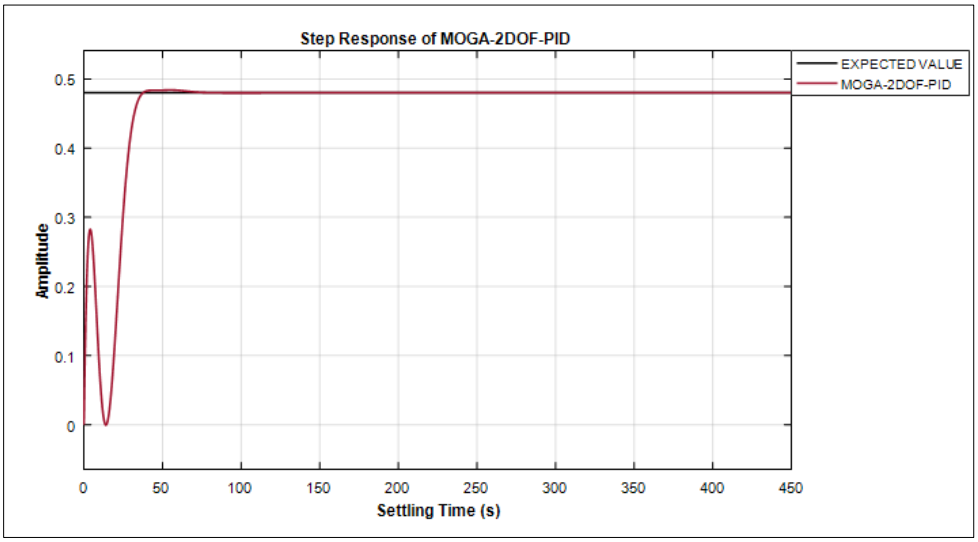

Figure 30 Step Response of MOGA-2DOF-PID (Proposed)

In this study, the simulation results are presented as bar graphs in Figures 31, 32, and 33. Figure 31 shows the fitness function values (IAE) for the optimized parameters of the 2-DOF-PID controller, based on the simulations presented in Tables 7 to Table 11. It is evident from the figures that the proposed MOGA algorithm with the IAE-based controller achieves the lowest values, demonstrating superior performance compared to all other algorithms evaluated.

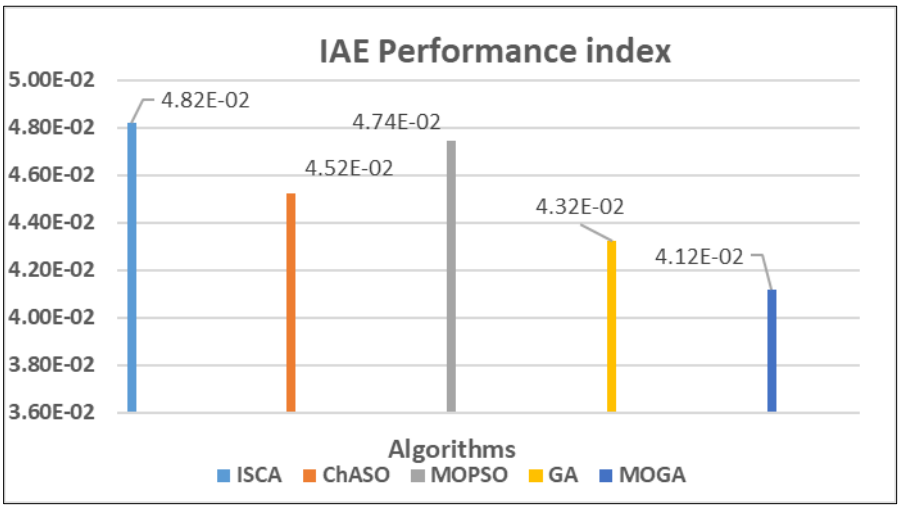

Figure 31 Comparison of IAE Performance index value

The fitness function values (ISE) for the optimized settings of the 2-DOF-PID controller, based on simulations from Tables 7 to Table 11 are presented in Figure 32. The figures clearly highlight the superior performance of the proposed MOGA algorithm, as the ISE-based error criteria for the controller yields the smallest error value, demonstrating the best performance among the compared algorithms.

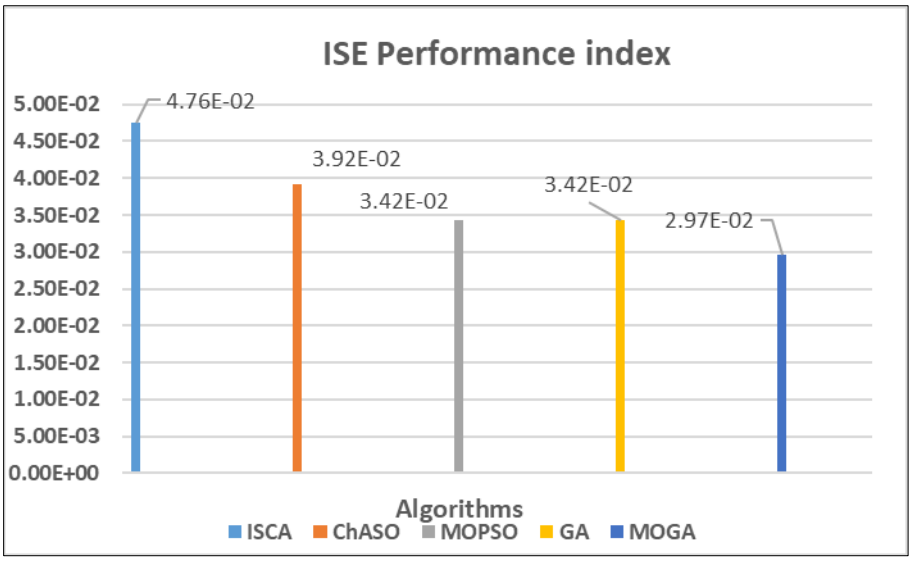

Figure 32 Comparison of ISE Performance index value

Figure 33 displays the fitness function (ITAE) values for the optimized parameters of the 2-DOF-PID controller, based on simulations from Tables 7 to Table 11, The results clearly indicate that, among all the compared algorithms, the proposed MOGA algorithm with ITAE-based controller achieves the lowest error values, demonstrating the best performance overall.

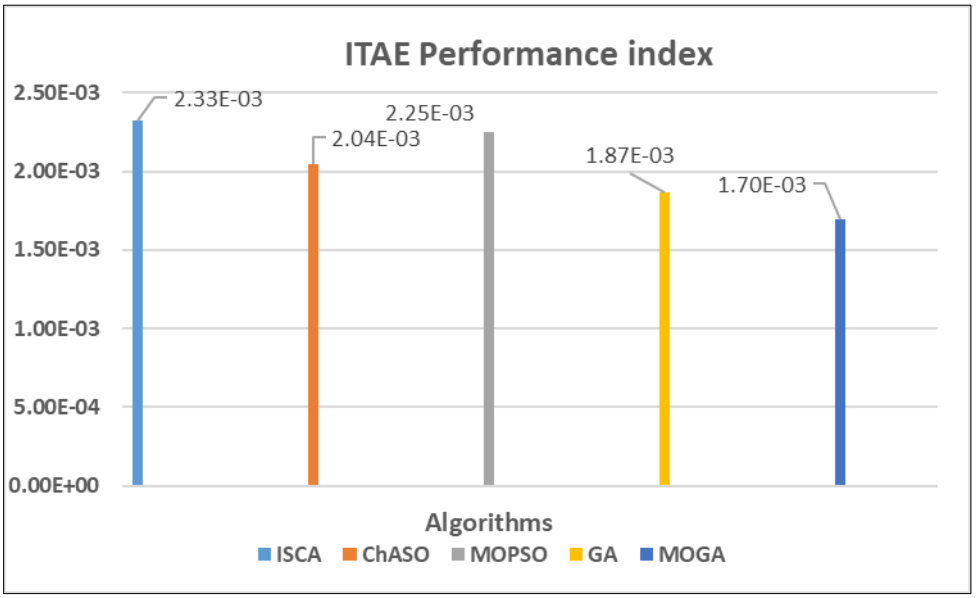

Figure 33 Comparison of ITAE Performance index value

From all the results obtained, it is clear that ITAE effectively minimizes larger errors when managing control systems with higher derivatives, regardless of the algorithm used. The results distinctly show that the MOGA-based ITAE approach achieves the smallest error (1.70E-03) when compared to the MOGA-based IAE (4.12E-02) and MOGA-based ISE (2.97E-02).

4.6. Comparison of Step Response of Air Pressure monitoring sensor with the five Algorithms

Figure 34 presents the combined overall step response of all the simulated algorithms featured in Figures 18, 21, 24, 27 and 30 respectively, providing a comprehensive comparison of their performance.

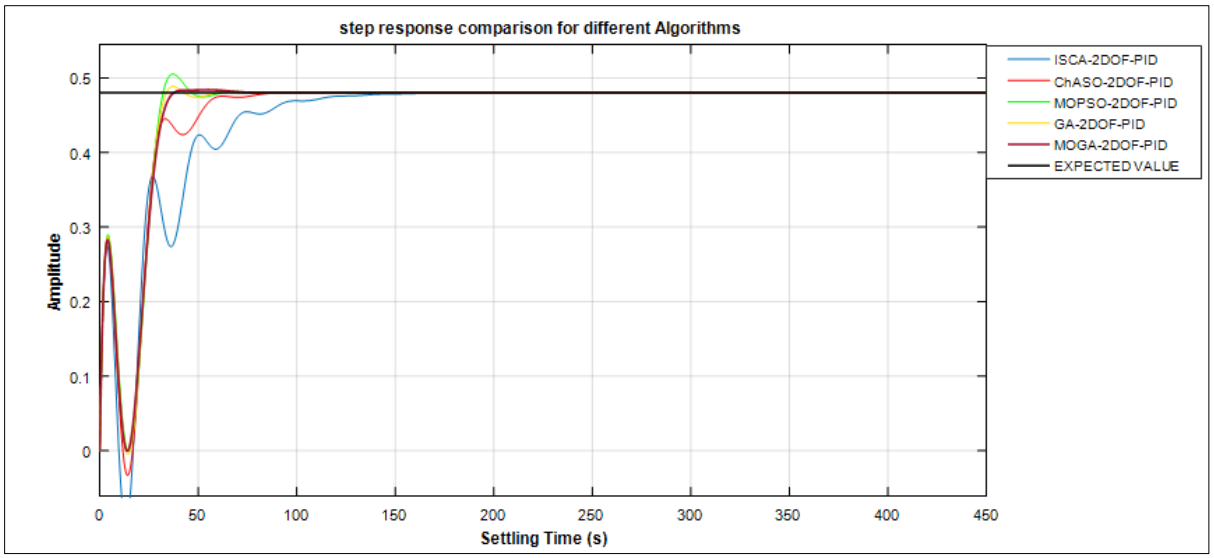

Figure 34 Step response comparison for different algorithms

Based on the results presented in the Table 12, it is evident that the proposed MOGA-2DOF-PID controller demonstrates superior performance compared to the other algorithms across several key time-domain response metrics. Notably, the MOGA-2DOF-PID achieves the shortest settling time of 44.25 seconds and the fastest rise time of 53.2 seconds, indicating its rapid and stable response to changes in input. It also maintains a minimal overshoot of just 1.24% and no undershoot, showcasing excellent control precision and stability. While MOPSO-2DOF-PID exhibits the highest peak value at 0.526, it also suffers from a significant overshoot of 8.33% and an undershoot of 11.4%, indicating a relatively unstable response. In contrast, the ISCA-2DOF-PID achieves the lowest peak value of 0.464 and no overshoot or undershoot, but this comes at the cost of a sluggish response, with the longest settling time of 143.84 seconds and rise time of 184.5 seconds. ChASO-2DOF-PID strikes a balance with a moderate peak value of 0.476, no undershoot, and a better settling time of 84.33 seconds, yet it is still outperformed by the MOGA-2DOF-PID in both response speed and overshoot control. GA-2DOF-PID performs relatively well with 0% undershoot, a modest overshoot of 2.46%, and respectable settling and rise times of 66.78 seconds and 79.3 seconds, respectively, but it also falls short of the performance achieved by MOGA.

Overall, the proposed MOGA-2DOF-PID controller leads across the majority of performance indicators, particularly excelling in fast response and stability, thereby confirming its effectiveness over the other optimization-based control strategies.

Table 12 Response performance for different algorithm based 2-DOF-PID controller

Algorithm	Peak Value	Overshoot %	undershoot%	Settling Time(S)	Rise Time(S)
ISCA-2DOF-PID	0.464	0	64.5	143.84	184.5
ChASO-2DOF-PID	0.476	0	45.5	84.33	147.2
MOPSO-2DOF-PID	0.526	8.33	11.4	98.34	88.5
GA-2DOF-PID	0.491	2.46	0	66.78	79.3
MOGA-2DOF-PID(Proposed)	0.485	1.24	0	44.25	53.2

4.7. Comparative Analysis of the Developed System with the Most Related Research

The outcomes of this research were compared with those reported by [25] to evaluate performance improvements. The comparison highlights that the proposed MOGA-2DOF-PID-based air pressure monitoring sensor control system demonstrates superior performance over the previously utilized algorithms. The enhanced results from the newly developed system, evaluated using Equation (14), clearly indicate significant improvements in control efficiency. The comparative analysis between the earlier study and the present work is illustrated below for better insight.

$$\% \text{ improvement} = \frac{Developed\ algorithm - Existing\ algorithm}{Existing} \times 100 \qquad (14)$$

Table 13 Comparative Analysis of the developed system with state-of-the-art

Metric performance	**[25] (Existing TOPSIS/MOSPO)**	**Developed Algorithm (MOGA)**	**% improvement**
Flow Rejection disturbance (%)	-33.4	-82.9	148.2
Temp. Rejection disturbance (%)	-72	-76.8	6.66
Rising Time (sec)	107	53.2	-50
Settling Time (sec)	143	44.25	-69
% Undershoot	0.02	0	-100
% Overshoot	4.8	1.24	-74.16
Peak Time (sec)	0.480	0.485	1.04

Table 13 highlights the superior performance of the newly developed control system when compared to the existing air pressure monitoring sensor system. Notably, it achieved a significant improvement in flow disturbance rejection by 148.2% and temperature disturbance rejection by 6.66%. Additionally, the system demonstrated a 50% reduction in rise time and a 69% decrease in settling time. It also effectively eliminated undershoot (a 100% reduction) and minimized overshoot by 74.16%, while achieving a quicker peak response time of just 1.04 seconds.

5. Conclusion

This study presents a comprehensive performance analysis of a 2DOF-PID controller optimized for an air pressure monitoring sensor system, employing a Multi-Objective Genetic Algorithm (MOGA) under three widely used control performance criteria: IAE, ISE, and ITAE. The research addresses a critical challenge in real-world control systems. time delays caused by sensor lag, actuator dynamics, or signal transmission which often degrade system stability and accuracy. To mitigate these issues, the system was modeled using a transfer function representing the dynamic behavior of the air pressure monitoring sensor, which plays a vital role in regulating pneumatic system operations. The introduction of a 2DOF-PID controller allowed for independent tuning of reference tracking and disturbance rejection, enhancing control flexibility. MOGA, alongside other metaheuristic algorithms such as CHASO, GA, MOPSO, and ISCA, was utilized to optimize controller parameters. By incorporating fitness criteria (ITAE, ISE, and IAE), the robustness and responsiveness of the system's step response were significantly improved. The MOGA-optimized controller achieved the highest performance metrics, including a peak flow disturbance rejection of -82.9%, temperature disturbance rejection of -76.8%, a minimal overshoot of 1.24%, no undershoot, a rapid settling time of 44.25 seconds, and a rise time of 53.2 seconds, with a peak response of 0.485. This signifies a substantial advancement in the stability and responsiveness of pneumatic control systems. However, the study is limited by the assumption of idealized plant models and simulation-based validation, which may not fully capture real-world uncertainties. Future work is recommended to explore real-time hardware implementation, robustness under varying environmental conditions, and the integration of adaptive or machine-learning-based tuning strategies to further enhance system adaptability and performance.

Compliance with ethical standards

Disclosure of conflict of interest

No conflict of interest to be disclosed.

References

[1] M. Papoutsidakis, V. De Negri,and A. Chatzopoulos, Avraam. (2019). SENSORS AND POSITION CONTROL METHODS FOR PNEUMATIC SYSTEMS. International Journal of Engineering Applied Sciences and Technology. 4. 478-485. 10.33564/IJEAST.2019.v04i05.069.

[2] R.C., Beremeh, F.O Adunola, J. S., Mommoh, A., Airoboman, S.O., Ibharunujele and D.A., Emmanuel. A Hybrid Optimization Scheme for Tuning Fractional Order Pid Controller Parameters for A Dc Motor. International Journal of Science and Research Archive (IJSRA). 2024, 13(02), 2779–2789. https://doi.org/10.30574/ijsra.2024.13.2.2291.

[3] P. Mohindru. Review on PID, fuzzy and hybrid fuzzy PID controllers for controlling non-linear dynamic behaviour of chemical plants. Artif Intell Rev 57, 97 (2024). https://doi.org/10.1007/s10462-024-10743-0.

[4] S. N. F. Nahri, S. Du, B. J. van Wyk, T. D Nyasulu TD. Time-Delay Estimation Improves Active Disturbance Rejection Control for Time-Delay Nonlinear Systems. Machines. 2024; 12(8):552. https://doi.org/10.3390/machines12080552.

[5] R. H. Subrata, G. Ferrianto Gozali and D. Endang. Computational and Intelligent Optimization tuning Method for PID Controller. Journal of Theoretical and Applied Information Technology. 2022, Vol.100. No 7. Pp. 2007 – 2017.

[6] I. A. Abbas, and M. K Mustafa. A review of adaptive tuning of PID-controller: Optimization techniques and applications. Int. J. Nonlinear Anal. Appl. 15 (2024) 2, 29–37. Int. J. Nonlinear Anal. Appl. 15 (2024) 2, 29–37

[7] ISSN: 2008-6822 (electronic), http://dx.doi.org/10.22075/ijnaa.2023.21415.4024 .

[8] N. Ajlouni, A. Osyavas, F. Ajlouni, A. Almassri, F. Takaoglu and M. Takaoglu. Enhancing PID control robustness in CSTRs: a hybrid approach to tuning under external disturbances with GA, PSO, and machine learning. Neural Comput & Applic (2025). https://doi.org/10.1007/s00521-025-11170-0.

[9] V. Sebastian, B. Diego and C. Oscar. (2024). Comparative Assessment of PID Controller Strategies for Nonlinear Systems with Time-Varying Parameters. 2024 IEEE ANDESCON. Pp. 1-6. 10.1109/ANDESCON61840.2024.10755663.

[10] S. B. Joseph, E. G. Dada, A. Abidemi, D. O Oyewola, B. M. Khammas. Metaheuristic algorithms for PID controller parameters tuning: review, approaches and open problems, Heliyon. 2022, 8(5) ISSN 2405-8440, https://doi.org/10.1016/j.heliyon.2022.e09399.

[11] R. Saadi, M. Y. Hammoudi, O. Salah, K. Laadjal, A. J. M. Cardoso. A Two-Degree-of-Freedom PID Integral Super-Twisting Controller Based on Atom Search Optimizer Applied to DC-DC Interleaved Converters for Fuel Cell Applications. Electronics. 2023; 12(19):4113. https://doi.org/10.3390/electronics12194113.

[12] A. N. Karanam, and B. Shaw. A new two-degree of freedom combined PID controller for automatic generation control of a wind integrated interconnected power system. Prot Control Mod Power Syst 7, 20 (2022). https://doi.org/10.1186/s41601-022-00241-2

[13] G. B. A. Modified 2-DOF Control Framework and GA Based Intelligent Tuning of PID Controllers. Processes. 2021; 9(3):423. https://doi.org/10.3390/pr9030423

[14] X. Cao, H. Yan, Z. Huang, S. Ai, Y. Xu, R. Fu, and X, Zou. A Multi-Objective Particle Swarm Optimization for Trajectory Planning of Fruit Picking Manipulator. Agronomy. 2021; 11(11):2286. https://doi.org/10.3390/agronomy11112286.

[15] G. Harsh, S. Prakash, N. Kashif, A. G. Ibrahim, H. Muhammad, Y. Narendra, S. Pankaj, G. Manoj and C. Laxmi. (2022). PSO Based Multi-Objective Approach for Controlling PID Controller. Computers, Materials & Continua. 71. 4409-4423. 10.32604/cmc.2022.019217.

[16] U. K. Nkalo, O. O. Inya, O. P. Ifeanyi, A. U Bola and D. I Ewean, A modified multi-objective particle swarm optimization (M-MOPSO) for optimal sizing of a solar–wind–battery hybrid renewable energy system, Solar Compass. 2024, Vol 12, ISSN 2772-9400, https://doi.org/10.1016/j.solcom.2024.100082.

[17] H. H Thakkar, H. Shukla, and P. K Sahoo. Chapter 2 - Metaheuristics in classification, clustering, and frequent pattern mining, Editor(s): Sushruta Mishra, Hrudaya Kumar Tripathy, Pradeep Kumar Mallick, Arun Kumar Sangaiah, Gyoo-Soo Chae, In Cognitive Data Science in Sustainable Computing,Cognitive Big Data Intelligence with a Metaheuristic Approach, Academic Press, 2022, Pages 21-70, ISBN 9780323851176, https://doi.org/10.1016/B978-0-323-85117-6.00005-4.

[18] M. A, Albadr, S. Tiun, M. Ayob and F. AL-Dhief. Genetic Algorithm Based on Natural Selection Theory for Optimization Problems. Symmetry. 2020; 12(11):1758. https://doi.org/10.3390/sym12111758.

[19] J. C. Bansal, P. Bajpai, A. Rawat, A. K. Nagar (2023). Advancements in the Sine Cosine Algorithm. In: Sine Cosine Algorithm for Optimization. SpringerBriefs in Applied Sciences and Technology. Springer, Singapore. https://doi.org/10.1007/978-981-19-9722-8_5

[20] J. Too and A. R. Abdullah (2020). Chaotic Atom Search Optimization for Feature Selection. Arabian Journal for Science and Engineering. 45. 10.1007/s13369-020-04486-7.

[21] S. Katoch, S. S. Chauhan, and V. Kumar. A review on genetic algorithm: past, present, and future. Multimed Tools Appl 80, 8091–8126 (2021). https://doi.org/10.1007/s11042-020-10139-6

[22] P. Kurukuri, M. R. Mohamed, P. Srinivasarao, J. K K. Dokala, D, Koteswararao, and P. Swamy (2022). Performance of 2-DOF PID Controller in AGC of Two Area Interconnected Power System Using PSO Algorithm. Proceedings of the 6th International Conference on Electrical, Control and Computer Engineering. pp.119-133. 10.1007/978-981-16-8690-0_12.

[23] D. Fister, I. Fister, I. Fister, and R. Šafarič, "Parameter tuning of PID controller with reactive nature-inspired algorithms," Rob. Auton. Syst., vol. 84, pp. 64–75. 2011.

[24] A. Sai Varun and R. Padma Sree, "Tuning of PID controllers for first order stable / unstable time delay systems with a zero," Int. J. Control Theory Appl., vol. 8, no. 3, pp. 985–994, 2015.

[25] N. K. Gupta, M. K Kar, and A. K. and Singh. Design of a 2-DOF-PID controller using an improved sine–cosine algorithm for load frequency control of a three-area system with nonlinearities. Prot Control Mod Power Syst 7, 33 (2022). https://doi.org/10.1186/s41601-022-00255-w.

[26] S. A. Haresh A and J. G. Jagrut. 'Multiobjective optimization of 2DOF controller using Evolutional and Swarm intelligence with TOPSIS 'International conference on Engineering/Heliyon, pp,1-7,doi; 10.116/j.heliyon.2019.e01410. 2019